Alma Mater Studiorum - Università di Bologna

DOTTORATO DI RICERCA IN

Ingegneria elettronica, telecomunicazioni e tecnologie dell'informazione

Ciclo XXXI

Settore Concorsuale: 09/F2 - Telecomunicazioni

Settore Scientifico Disciplinare: ING-INF/03

LONG RANGE LOW POWER WIRELESS COMMUNICATION TECHNOLOGIES FOR THE IOT

Presentata da: Luca Feltrin

Coordinatore Dottorato
Prof.ssa Ing. Alessandra Costanzo

Supervisore
Prof. Ing. Roberto Verdone

Co-Supervisore
Ing. Chiara Buratti

Esame finale anno 2019

ABSTRACT

The Internet of Things (IoT) addresses a huge set of possible application domains, requiring both short- and long-range communication technologies. When long distances are present, a number of proprietary and standard solutions for Low Power Wide Area Networks (LPWAN) are already available. Among them, LoRaWAN and NB-IoT are candidate technologies supported by many network operators. This thesis discusses their possible role for the IoT.

LoRaWAN is one of the first technologies defined to operate in unlicensed bands. Devices employing it are already on the market, and many organisations are starting using them to design their own IoT projects. Its simple access protocol is designed to avoid complexity and costs and to minimise the energy consumption while maximising the transmission range. At the same time, the proprietary modulation used is very robust with respect to the interferers present in the shared bands used.

NB-IoT is a new radio access technology targeting a large set of use cases for massive machine-type communications standardised by the 3GPP. Similarly to LoRaWAN, NB-IoT has been enhanced in terms of coverage and power saving capabilities while reducing the complexity at the same time.

In this thesis, first, many typical applications that may benefit from these technologies are presented, with a focus on the performance metrics and the definition of the scenario and traffic pattern. Secondly, the LoRaWAN technology is assessed both experimentally and through simulations, to characterise it from the link-level and system-level viewpoint, with the target of estimating the capacity of a LoRaWAN gateway and a multi-gateway network to serve a large area. Then, this thesis provides an overview of NB-IoT, together with a mathematical model of the network able to predict the maximum performance in a given scenario with a specific configuration of some design parameters. This model is used to study how these parameters affect the overall performance and how the optimal configuration

may be chosen according to arbitrary criteria. Finally, some projects and practical activities are presented to prove the need for these standards, and to share the know-how that was developed during these studies.

Table of Contents

List of Figures

List of Tables

Glossary

3GPP	3rd Generation Partnership Project
ACK	Acknowledgement
ADR	Adaptive Data Rate
AS	Application Server
BSR	Buffer Size Report
BW	Bandwidth
CRC	Cyclic Redundancy Check
CRS	Cell-specific Reference Signal
D2D	Device to Device
DCI	Downlink Control Information
DL	Downlink
DR	Data Rate
DRX	Discontinuous Reception
ED	End Device
eDRX	extended DRX
eMBMS	Evolved Multimedia Broadcast Multicast Service
eNB	evolved Node Basestation
GPRS	General Packet Radio Service
GPS	Global Positioning System
GSM	Global System for Mobile Communications
GSMA	GSM Association
GW	Gateway
HARQ	Hybrid Automatic Repeat reQuest
HTTP	HyperText Transfer Protocol
IoT	Internet of Things

IP	Internet Protocol
ISD	Inter-Site Distance
ISM	Industrial, Scientific and Medical
JS	Join Server
LoS	Line of Sight
LPWAN	Low Power Wide Area Network
LTE	Long Term Evolution
MCL	Maximum Coupling Loss
MCS	Modulation and Coding Scheme
MIB-NB	Narrowband Master Information Block
mMTC	massive Machine Type Communication
MQTT	Message Queue Telemetry Transport
NACK	Not Acknowledgement
NCCE	Narrowband Control Channel Element
NCellID	Narrowband Cell ID
NDI	New Data Indicator
NPBCH	Narrowband Physical Broadcast Channel
NPDCCH	Narrowband Physical Downlink Control Channel
NPDSCH	Narrowband Physical Downlink Shared Channel
NPRACH	Narrowband Physical Random Access Channel
NPSS	Narrowband Primary Synchronization Signal
NPUSCH	Narrowband Physical Uplink Shared Channel
NRS	Narrowband Reference Signal
NS	Network Server
NSSS	Narrowband Secondary Synchronization Signal
OFDM	Orthogonal Frequency-Division Multiplexing
PDCCH	Physical Downlink Control Channel
PLMN	Public Land Mobile Network

PRB	Physical Resource Block
PSM	Power Saving Mode
RA	Random Access
RAP	Random Access Procedure
RAR	Random Access Response
RE	Resource Element
RNTI	Radio Network Temporary Identifier
RRC	Radio Resource Control
RSSI	Received Signal Strength Indicator
RU	Resource Unit
SC-FDMA	Single Carrier Frequency Division Multiple Access
SC-MRB	Single Cell Multicast Radio Bearer
SC-PTM	Single Cell Point to Multipoint
SF	Spreading Factor
SIB-NBs	Narrowband System Information Blocks
SIB1-NB	Narrowband System Information Block 1
SIB2-NB	Narrowband System Information Block 2
SINR	Signal to Interference plus Noise Ratio
SIR	Signal-to-Interference Ratio
SNR	Signal to Noise Ratio
TAC	Tracking Area Code
TAU	Tracking Area Update
TBS	Transport Block Size
TCP	Transmission Control Protocol
TTI	Transmission Time Interval
UAV	Unmanned Aerial Vehicle
UCI	Uplink Control Information
UDP	User Datagram Protocol

UE User Equipement

UL Uplink

VIP Very Important Person

Symbols

A	first coverage model tuning coefficient
A_c	number of RA attempts
B	second coverage model tuning coefficient
β	Okumura-Hata path loss exponent
c	coverage class ($c \in \{N, R, E\}$)
d	deployment condition ($d \in \{O, I, DI\}$)
r	distance in kilometers
G_{tot}	arithmetic sum of all the antenna gains, cable and other sources of losses in dB
JI	Jain's fairness index
K	Okumura-Hata path loss at one kilometer in dB
L	path loss in dB
L_{add}	additional path loss due to indoor deployment
λ	device packet generation rate (packets per day)
N	number of devices
N_{max}	network size
N_{RU}	number of RUs needed for the transmission of a given Payload
O	offered traffic (packets per day)
O_{max}	network capacity (packets per day)
$p_{c,d}^{CLASS}(r)$	probability of choosing coverage class c
$p_{c,e}^{\mathrm{CONN}}$	connection probability
$p_{c,d}^{\mathrm{COV}}(r)$	coverage probability
p_d	deployment condition probability
$P_{e,max}$	maximum error rate
P_L	payload size (bytes per packet)

p_c^{MAC}	network access success probability
P_{r0}	received power at one kilometer in dBm
P_s	success probability
P_t	transmit power in dBm
α	protection ratio
R_c	number of repetitions used in all physical channels
R_{cell}	cell radius
$R_{\min}$	number of repetition required
ρ	number of devices per square kilometer
ρ_{UL}	uplink occupation coefficient
S	log-normal shadowing in dB
S_c	number of subcarriers allocated for the NPRACH
σ_S	shadowing standard deviation
T	network sum throughput (kbps)
T_c	periodicity of the NPRACH occurrence
T_{max}	maximum network throughput possible with a certain configuration
τ_p	preamble duration
Th_c	coverage class decision thresholds ($Th_3 = -\infty$)
T_A	time on air
Z_c	capacity of the NPRACH in preambles per second

Chapter 1

Introduction

The Internet of Things (IoT) is emerging as a set of integrated technologies, new solutions and services, which are expected to change the way people live and produce (or benefit from) goods. The IoT paradigm, making all unmanned "things" (daily objects, industry machines, sensors, robots, animals, etc.) connected to the Internet, addresses a very large set of application domains. Some of them require short-range radio communication technologies (like Zigbee), being the network nodes confined in restricted areas; others, like precision agriculture, environmental monitoring, or animal tracking, may require communication solutions able to cover distances up to (or more than) 10 km in rural areas. Recently, the interest of industry towards the latter category, denoted as Low Power Wide Area Network (LPWAN), grew significantly [9]. The extended transmission range is not the only peculiar requirement of these applications, devices are expected to generate a very sporadic traffic whereas the market trends show that the number of devices active simultaneously in the territory will be extremely high; in this case I denote with massive Machine Type Communication (mMTC) the applications requiring a high device density.

The effective support of these applications [10] is expected to play a key role in the market of IoT for the emerging 5G ecosystem [11]. The unique requirements in terms of coverage, battery life, and device complexity of mMTC dictated an ad-hoc design of wireless technologies [12].

Some proprietary solutions, working on license-exempt spectrum bands such as Industrial, Scientific and Medical (ISM) bands at 433 and 868 MHz, are already deployed in some regions: as an example, Sigfox operates both as a technology and a service provider for LPWAN; another big player is the LoRa Alliance, which

was officially established in Mobile World Congress 2015 and produced a proprietary solution known as LoRaWAN working in the license-exempt band, available in many countries.

Meanwhile, the 3rd Generation Partnership Project (3GPP) is supporting three different LPWAN standards that will work on the licensed spectrum of mobile networks: Extended Coverage Global System for Mobile Communications (GSM) (EC-GSM-IoT), Long Term Evolution (LTE) Machine Type Communications Category M1 (LTE-MTC Cat M1) and Narrowband IoT (NB-IoT). The latter technology has technical characteristics similar to LPWAN proprietary solutions, with the advantage of being a standard; many mobile network operators worldwide are supporting the development of NB-IoT, which might become a future reference IoT communication technology for several application domains. In the meanwhile, some network operators are pushing the LoRaWAN technology and supporting the developers' community [13].

In this context, made of many evolving technologies, it can be expected that a single one will not be capable of addressing efficiently all the different IoT use cases. It is in the interest of big players, to identify the range of applications that make a specific technology suitable. This thesis shows results of an ongoing project developed at the University of Bologna and supported by Telecom Italia Mobile, aimed at defining the technical limits of two of the aforementioned technologies, LoRaWAN and NB-IoT, and the opportunities they provide from both a link- and system-level points of view.

The remainder of this thesis is organised as follows: Chapter 2 presents the mathematical and conceptual background for the later analysis, more specifically the assumptions on the channel and traffic models and a detailed description of typical LPWAN use cases. Chapter 3 consists in a description of the LoRaWAN technology and a series of link-level and system-level analysis performed through experiments and simulations. Chapter 4 consists in a detailed description of the NB-IoT standard and of a mathematical model developed to estimate system-level performance metrics. In Chapter 5 I summarise some practical applications and testbeds I de-

veloped during the last three years in order to provide some insight on the technical issues related to the use of LoRaWAN. Finally, in Chapter 6 I draw some conclusions and I propose a series of activities that may be a natural continuation of this research activity.

Chapter 2

LPWAN Use Cases

As discussed in Chapter 1, in the next years many new technologies for the IoT and LPWANs will be defined.

A wider set of technologies available, each of them designed to optimise the performance of the network in a specific case, will allow the coexistence of a similarly large set of heterogenous applications and systems. It will be up to the operator, the user, or any kind of intelligence, to choose the most appropriate one given the current status of the network and the type of service required.

Understanding which technology is more suited for a particular application becomes a major challenge in such design framework; thus a systematic method to predict the network performance could be of major interest.

The remainder of the chapter is organised as follows: in section 2.1 the reference scenario, from the propagation to the geometrical point of view, is presented with the related assumptions; the metrics of interest to describe the traffic, the behavior of the devices and the method to evaluate the network performance are presented in section 2.2. In section 2.3 a list of reference use cases is presented. Finally, in section 2.4 a grouping criterion is defined in order to motivate the choice of performing the following analysis only on a subset of use cases.

2.1 Reference Scenarios

In order to produce realistic results from the analysis of these standards and applications, the deployment scenario should be defined properly.

From the electromagnetic point of view, the modeling of the signal propagation has been widely addressed in the literature. Usually the devices of interest are deployed at ground level and they are served by a cellular-like network. The environment where the devices are deployed may be in the range of a dense urban scenario to a rural area. Moreover, in some cases, we consider also devices deployed indoor or in deep-indoor conditions (such as water or gas meters). In such difficult coverage conditions we consider an additional path loss denoted as L_{add} which normally can be up to 40 dB.

The simplest statistical model of the channel loss in such conditions is the Okumura-Hata model. This model, described in [3], provides the average path loss, due to propagation only, as a function of several parameters, such as the carrier frequency, the height of both the transmitter and the receiver, and their distance. Also, depending on the environment being urban, suburban or rural, it provides different expressions for deriving the final result.

Regardless of the exact formulation of the model, the expression of the path loss can be simplified as in Equation 2.1 where L is the propagation path loss in dB, K is the path loss at one kilometer in dB, β is the path loss exponent, and r represents the distance between the transmitter and the receiver in kilometers. This expression summarises the dependency of the coverage from the distance, whereas the other parameters, once a technology and an environment has been defined, are fixed.

The two parameters K and β can be derived using the Okumura-Hata model itself, or they can be derived experimentally as it is done in some parts of this thesis.

$$L = K + 10\beta \log(r) \tag{2.1}$$

Table 2.1 reports the values of these parameters for the different environments considered by the Okumura-Hata model, assuming to have a base station located at 30 meters of altitude and a mobile terminal at 1.5 meters of altitude.

We also assume to have variations of the signal strength only due to shadowing effects; these variations can be modeled as a log-normal attenuation, denoted as

S, with average 0 and a given standard deviation, denoted as σ_S, which depends on the environment characteristics. The Okumura-Hata model does not predict a value for this parameter; in Table 2.1 I considered values of σ_S which are realistic based on our experience, considering that for most of the applications there is a very low mobility and thus a very static environment.

For what concerns cellular networks and urban scenarios, 3GPP already studied the statistics of the path loss and it provides the value of the aforementioned parameters for the city of London and for the 900 MHz cellular band. These values are reported as well in Table 2.1. [2]

Finally, the last row of Table 2.1, represents the parameters which were derived experimentally by placing a device on top of a 240 meters high hill and a mobile terminal at 1.5 meters from the ground around the city of Bologna. Further details about this experiment are provided in Chapter 3. During this experiment it was made sure the first Fresnel ellipsoid was free from obstacles, allowing Line of Sight (LoS) conditions.

Finally, I provide a general expression for the received signal power in dBm as a function of distance. This will be used through this thesis and it considers all the aforementioned aspects and parameters. This expression is shown in Equation 2.2 where P_t is the power of the transmitter in dBm, G_{tot} is the arithmetic sum of all the antenna gains, cable and other sources of losses in dB, P_{r0}, equal to $P_t + G_{tot} - K$, is the received power at one kilometer in dBm. These parameters depend on the technology considered and their values will be provided in the dedicated chapters.

$$P_r(r) = P_{r0} - 10\beta \log(r) - S - L_{add} \tag{2.2}$$

Another important aspect related to the deployment scenario is the distribution of users across the served area.

Usually, the users are considered to be deployed uniformly in the area under investigation with a certain density. Regarding the urban scenario, in Table 2.2 it is reported the average number of households per square kilometer as defined by

Environment	K	β	σ_S
3GPP London	120.9	3.76	8
Okumura-Hata urban	126	3.52	8
Okumura-Hata suburban	116	3.52	8
Okumura-Hata rural	98	3.52	2
LoS measurements	86	2.93	2

Table 2.1: Definition of channel model for different environments [2, 3].

3GPP in [2] and [4]. Depending on the application considered, there may be a different number of devices per household. For example, in metering applications one device per household may be considered, while for domotic applications tens of devices per household is more appropriate.

In general, not all the applications imply a device density dependent on the number of households, even though there may be a correlation between the two. In general I denote with ρ the average number of devices per square kilometer deployed in the area of interest. This information, when available, is reported in Table 2.6 for what concerns the use cases described in [6].

One of the key aspects of LPWANs is a design characterised by low complexity and thus low costs. In order to keep the overall system complexity as low as possible, the protocol implemented should be simple as well as the topology of the network. Usually, the topology considered is a star. A star topology consists in a central device called "sink" which usually coordinate the network, collects data from the other devices or transmit to them, the other devices are peers and directly connected only to the sink. When an area to cover is very large many sinks may be deployed, the architecture of the system is the same of cellular networks where every device is connected only to one sink, usually the one with the most favorable channel.

2.2 Metrics

Our analysis is focused on the network performance, therefore it is important to define the type of traffic that is generated by the devices connected to the network

	Tokio	London
Urban	2316	1517
Dense Urban	7916	4275

Table 2.2: Households per square kilometers in Tokio and London [4].

itself. The metrics mentioned in the reminder of this section are summarised in Table 2.3.

Differently from legacy network traffic, where users typically download large files or require a continuous streaming of data, for the applications of our interest the devices transmit small amounts of data sporadically. In fact, since energy consumption is one of the aspects that should be minimised in LPWANs, the devices remain silent for most of the time; they turn on only to transmit their data or to perform some sort of synchronization with the network. Typically the packet generation time per node, denoted as λ, can be from a packet every ten minutes down to a packet per day.

Assuming each device generates packets with a uniform distribution over time, the traffic is defined with two metrics: the offered traffic O, or in other words the average packet rate of all the devices combined, and the payload size P_L that expresses the number of bytes sent in each packet.

Due to the sporadic behavior of each device, and given the large number of devices that we target in the use cases of interest, the device acting as a sink will receive a multitude of uncorrelated packets from different sources. Under this assumption, it does not really matter if the packets are generated by devices transmitting very sporadically, or by less devices transmitting more often, what actually impacts the performance is the total number of packets per unit of time transmitted concurrently. The duration, or the amount of data to transmit each time, has also an impact on how many radio resources should be used to serve the connected devices. This consideration motivates the choice of considering only the offered traffic and the payload size to define the traffic behavior.

A use case is defined not only by the traffic pattern generated by the devices, but

also by the requirements on the perceived performance that should be satisfied.

One of the main metric taken into consideration is the success probability, denoted as P_s. This metric expresses the probability for a generic node to transmit correctly a packet to the network. It considers the radio coverage of the devices, as the further they are from the sink the more difficult is to serve them, and also the radio channel access protocol effectiveness, as more complex mechanisms allow more transmission to be scheduled in the same amount of time. Usually the error rate should be smaller than a maximum requirement, denoted as $P_{e,max}$, which represents the reliability needed for a transmission. Usually for LPWAN applications it is not expected to have a very reliable communication, in some cases it is acceptable to lose even 10% of the packets.

Another important metric taken into consideration is the network throughput, denoted as T. This metric expresses the amount of data that is successfully transmitted in the network per unit of time; it should be higher than a minimum requirement. It is strictly related to the success rate as the amount of data transmitted is simply the amount of traffic generated multiplied by the probability of success. In fact the relation expressed in Equation 2.3 connects these two metrics and some of the aforementioned parameters. The division for the constant $8.64 \cdot 10^7$ is necessary to match the unit of measures of the parameters defined, it is defined as $\frac{s \cdot bps}{day \cdot kbps}$.

$$T = \frac{8OP_LP_s}{8.64 \cdot 10^7} \tag{2.3}$$

In LPWANs it is important to define also a requirement in terms of energy consumption. Usually this metric is expressed in years of battery lifetime, assuming a battery with a certain initial energy. Apart from hardware related design challenges, this metric involves the possibility for a device to work with a very low duty cycle, spending most of the time in power saving mode with the transceiver turned off.

One of the main challenges of LPWANs was to extend the transmission range of the devices; in terms of coverage, an extension of 20 dB with respect to General Packet

Radio Service (GPRS) capabilities was required, bringing the Maximum Coupling Loss (MCL) up to 164 dB. A generic use case may require the deployment of devices in areas with poor coverage (very far from the sink or in basements) where such high MCL is required.

The low energy consumption and the long range of transmission are mostly obtained by reducing the nominal bitrate of the transmission and the duty cycle. This implies a dilation of all the timings related to the communication. For the use cases of interest this often is not a problem as the very low update frequency allows to have a longer latency since the moment the data is generated to the moment it is received correctly. The requirement on the latency will be, then, more relaxed compared to other applications. Nevertheless, some of the use cases presented afterwards require a very strict latency constraint, in the order of few milliseconds. In these cases LPWAN technologies are not suited for this and only the evolution of cellular networks into 5G can satisfy the requirement.

As mentioned in section 2.1, it is expected to have a very high number of devices deployed in the area. Also, it is expected to have a larger area covered by a single sink due to the improved coverage capabilities. Therefore the minimum number of connected devices per cell, another metric of interest, should be higher compared to other technologies. For the same reason, one of the metrics estimated in the remainder of this thesis is the maximum number of devices that can be connected at the same time to a sink or cell.

Finally, another important metric considered is the Jain's fairness index, denoted as JI. This metric estimates the fairness of the service provided to all the users; in other words, whether they experience the same quality of service or not. According to the definition of Jain's index, reported in Equation 2.4, the individual throughput of each device is considered. Ideally, if all the devices transmitted with the same throughput, the Jain's Index would be 1. The total number of devices is denoted

with N while the individual throughput of the i-th node is denoted with t_i.

$$JI = \frac{\left(\sum_{i=1}^{N} t_i\right)^2}{N \cdot \sum_{i=1}^{N} t_i^2} \tag{2.4}$$

3GPP defined a set of requirements related to some of the aforementioned metrics, which were used to define cellular based massive IoT technologies. These requirements are reported in Table 2.4.

2.3 Use Cases

Many possible applications and scenarios have been studied and defined in the literature. All of them can be grouped in macro categories based on the industrial field of origin or based on similar characteristics.

We selected two documents containing information about typical LPWAN use cases which I will consider throughout the remainder of this thesis. The white paper [5] has been elaborated by the GSM Association (GSMA) to analyze licensed spectrum-based technologies and to analyze the key applications and services which might be implemented with these technologies. In this section I focus on the latter, which includes a detailed description of the applications with an estimation of some of the aforementioned metrics.

The second document is [6], a technical report elaborated by Ericsson addressing the current evolution and trends on the cellular traffic and providing an insight on IoT and mMTCs. The report presents, similarly to the previous one, some use cases and details on the device distribution and their generated traffic.

Table 2.6 summarises all the use cases presented in the next sections.

Symbol	Description	Unit of Measure
λ	Device Packet Generation Rate	packets/day
O	Total Offered Traffic	packets/day
P_L	Payload Size	bytes
P_s	Success Probability	-
T	Network Throughput	kbps
-	Average Device Battery Lifetime	years
MCL	Maximum Coupling Loss	dB
-	Average Latency	seconds
N_{max}	Maximum Number of Connected Devices	-
JI	Jain's Fairness Index	-

Table 2.3: Summary of the metrics of interest.

Metric	Requirement	Unit of Measure
Minimum battery life	10	years
Coverage improvement w.r.t. GPRS (MCL)	20 (164)	dB
Maximum latency	10	seconds
Minimum throughput	160	bps
Minimum number of connected devices per cell	52500	devices/cell

Table 2.4: 3GPP LPWAN use case requirements. [2]

2.3.1 Smart Cities

One of the most important sets of applications for IoT, addresses the problem of enhance the automation of cities. Many infrastructures providing services to the citizens can be optimised using IoT technology in order to be more efficient both in terms of quality of service provided and resources consumed.

The most common example is the metering of utilities consumption, such as electricity, water or gas. In Italy, for instance, the electricity metering is already controlled remotely through power line technology, but operators are planning to upgrade the meters with a secondary radio interface to increase the redundancy of these devices. On the other hand, gas and water meters are still disconnected from the internet; the use of LPWAN technologies could improve the process of reading and pricing these consumptions. This is one of the few use cases addressed by both [6] and [5], and they agree on the size that a packet generated by a meter should have, 100 bytes. Depending on the specific supply monitored, a device may transmit from one to 48 packets per day. It is expected to have up to ten thousands devices per square kilometers in a urban scenario. Usually the devices will be deployed indoor

or deep-indoor, so the coverage is an important aspect to consider. Even though an electricity meter may be plugged to a power source for obvious reasons, a water and gas meter may be battery powered. Latency is not a strict requirement in this case and up to a minute it is acceptable.

In order to optimise the vehicular traffic flow in a city, it can be possible to monitor all the parking spots in order to provide to the drivers direction to the closest free one, potentially through an app installed on their smartphones. This application is called smart parking. Every device, deployed mostly outdoor but in some cases indoor or deep-indoor, should send an update composed of 50 bytes relatively often, up to 60 times per day. In fact the transmission of a message could be activated only when a change of status is detected. The density of devices and parking spots, depends largely on the size of the city considered and whether private parking buildings are considered or not. As a reference, in Santander (Spain) a testbed for IoT applications employing 802.15.4 standard has been deployed involving also smart parking applications [7]. They distributed 400 sensors in an urban area of 0.13 km^2, making the average density of devices around 3000 per km^2. The maximum latency can be in the order of one minute.

Another interesting application is waste management; the idea is to equip trash bins around the city with sensors to detect how full they are in order to plan their emptying and minimise the effort for this task. In this case the devices are battery powered, but the lifetime required could be quite short since the collection of wastes is scheduled almost daily, thus the operators may replace the batteries very often. The devices will be deployed mostly outdoor. Regarding the traffic pattern, it is expected to receive an update consisting of few bytes once every hour. Again, the latency is not a strict requirement, thus a minute can be considered as the maximum.

In a smart city also the functioning of the illumination system can be controlled and optimised. Light poles can be equipped with sensors able to detect the presence of people or cars in order to turn on the light only when it is needed, saving a considerable amount of energy. In this case the sensors could be deployed mostly

outdoor and plugged to a power source. The devices are mostly autonomous, but they could receive commands from the network or report about their status in a very sporadic way. It is estimated that it is needed to transmit five packets composed of 100 bytes per day. The latency normally is not a tight constraint, but there are some variations of this use case that may require a faster message delivery: for example, a lamp pole could blink in order to guide an ambulance to the location of an emergency.

Finally, also the power grid, distributing energy throughout the city, can be managed remotely. The distribution grid has a hierarchical structure, as we move towards the high and extra-high voltage domain, the area to cover becomes larger. It is expected that each device transmits ten packets per day, each of them composed of 20 bytes. This application requires also to control directly the power grid in case of emergency or sudden changes of load. For this reason the latency requirement should be more stringent, in the order of one second. Depending on the deployment with respect to the grid architecture, the devices may be plugged to a power source or equipped with a battery.

2.3.2 Environmental Monitoring

Another field which can get a great benefit from IoT, and in general automation, is environmental monitoring or, in other words, the monitoring of several variables related to the environment in order to produce statistics, estimate quality indicators or detect hazardous events.

In order to monitor the trend of environmental variables (such as temperature, vibrations or pollution) many sensors can be deployed in the area of interest. They will perform periodical measurements followed by the transmission of the outcome to the cloud. We define this use case as “Data Collection”. The traffic pattern depends much on the kind of variable to monitor and in particular its variations; nevertheless, the transmission of packets is very regular and continuous. We consider a transmission of 200 bytes every hour. One of the key aspects of this use

case is the energy requirement. In fact, the devices will be most probably deployed in remote locations where it is difficult for an operator to reach to perform maintenance or replace the battery; therefore, the lifetime considered is in the order of tens of years. For the same reason, even through the devices will be deployed mostly outdoors, they will be considerably far from the network infrastructure, so coverage can be a major problem. On the other hand it is expected to have a sparse distribution of devices in the area. Normally both the reliability and the latency requirements are not very tight.

In similar scenarios it is possible also to monitor the status of the environment and raise an alarm only when an hazardous situation is detected, for example in case of a fire in a forest. In this case the transmission of packets will be much less frequent, only to report the status of the device itself, but once an alarm is transmitted it should reach the destination with a very reliable communication and quickly.

Another important field for this kind of applications is smart agriculture. The precise monitoring of plants status can lead to a more efficient use of the natural resources such as water, and let the operators act faster in case of a spreading disease. Due to the slow variations of the health status of the plants, it is still possible to transmit a report with a very low rate, 100 bytes every 6 hours. Again, the devices will be most likely battery powered and deployed outdoor, the other requirements are similar to the data collection use case.

Finally, another application related to smart agriculture, is the monitoring of cattle. Devices equipped with a Global Positioning System (GPS), or other localization technologies, can control the current position of the animals, raise an alarm, or discourage the movement of the animal in that direction once the animal reach the limit of a given area. In other words implementing a geofencing system. Also, the devices could monitor other variables related to the health of cattle or detect ovulation in order to optimise the breeding process. In this case the devices are moving terminals, therefore the network should react dynamically to the changes of the channel, even though its coherence time could be very high. In order to implement a close-to-real-time application, the packet rate should be much higher,

e.g. 50 bytes to be transmitted 100 times per day.

2.3.3 Smart Buildings

IoT can also improve the automation and safety of buildings through the use of smart devices.

A classical example of application dedicated to buildings is home automation: various kinds of sensors and actuators can be equipped with radio transceivers in order to control remotely the health status inside a building, optimise the energy consumption and allow users to remotely control their house. The traffic pattern strongly depends on the kind of sensors or actuators considered; in the aforementioned documents it is estimated that five packets composed of 50 bytes, may be transmitted every day, on average, for monitoring purposes. The devices will be deployed indoor or, in some cases, deep indoor, while the energy constraints may be more relaxed as many devices could be plugged to a power source. For monitoring purposes the latency is not a tight requirement, as usual, but in some case a command to an actuator (e.g.: turning on/off a light) should be transmitted with no perceivable latency (less than 100 ms).

Similarly to the environmental monitoring group of use cases, there can be an application where devices detect hazardous conditions and raise an alarm, for instance smoke detectors. Few packets per day may be transmitted to notify a device is still alive and connected, but in case of a fire the alarm should be transmitted very reliably and with low latency. Of course in this case, differently from event monitoring use case, the devices will be deployed indoor or deep-indoor.

Another interesting application belonging to the category of smart buildings is microgeneration. A microgeneration plant has the target of locally generate and provide heat and power to the building with small scale equipment. Typically, this use case involves photovoltaic cells, solar panels, wind turbines and other devices, deployed on the building roof. The precise monitoring of the energy produced by this equipment can help optimise the energy distribution on a larger scale. The

devices will be deployed mostly outdoor on roof tops, and they could be plugged to a power source. The traffic pattern is regular, for instance 100 bytes sent twice per day.

2.3.4 Industry 4.0

Another field that could take many benefit from IoT is industry. In fact, the set of the many possible applications in this field, denoted as Industry 4.0, consists in very different requirements. In particular, the requirement for the latency make some application suitable for LPWANs, some other even impossible with the current level of technology. It is expected to satisfy these requirements with the 5G cellular network.

An example of traditional LPWAN application is asset tracking where, through an indoor or outdoor localization system, it is possible to track the current position of various assets. For this kind of application it is required a reasonably high refresh rate, which could be 100 times a day by sending 50 bytes. Nevertheless, the requirement on latency will be the typical one for the use cases discussed, in the order of 30 seconds. The devices could be deployed outdoor or indoor, depending on the type of industry involved, and most likely they will be equipped with a battery or energy harvesting systems.

A similar use case is gas tank monitoring, a very specific application where pressure, temperature and other variables related to the status of a gas, are monitored in order to detect hazardous situations. The traffic pattern is expected to consist in 2 packets composed of 100 bytes sent every day to notify about the status of charge of the device and statistics of the gas. The transmission should be reliable even though the latency expected can be in the order of one minute due to the small packet rate. In case of an hazardous situation the packet should be delivered with a higher reliability and lower latency in order to react quickly.

Finally another scenario representative of Industry 4.0 is machinery control. In this case we have to distinguish two different aspects of the same application. In fact,

the innovation comes from the idea of controlling the machines at a very low level, especially controlling directly the hundreds of analog signals that are sampled and used in control loops to activate the actuators. Transmitting this kind of signals through radio transceiver require a reasonably wide bandwidth and very low latency; in fact, it should be lower than ten milliseconds. Currently it is not possible to reach such low latencies with the current technologies. It is expected, though, that with 5G the minimum latency could be shortened in order to satisfy this requirement. Nevertheless, this application remains widely out of the capabilities of LPWAN technologies despite being a mMTC application. On the other hand, the overall process involving machines could be controlled and monitored using the technologies of our interest and with other requirements. Up to 100 packets per day could be delivered by the devices deployed indoor in very difficult propagation environments.

2.3.5 Consumer

A very wide set of use cases is based on consumer electronics; countless devices and applications are expected to be utilised by the average customer.

The first example is represented by wearable devices, such as smartwatches, which can provide information on heartbeat, position or others to the user's smartphone or directly to the cloud. The energy constraints are not particularly tight as the user is in contact with the device every day and he/she may replace the battery on a weekly or monthly basis.

Another kind of devices which can be equipped with radio transceivers are white goods. They include all the household appliance such as refrigerators, air conditioning systems and stoves. Being connected to internet, they could implement a wide number of applications and services and improve the automation of the house in general. Deployed normally indoor, these devices may generate a very sporadic traffic containing updates on the current status of the variables or items monitored. In this case it is expected the devices to be plugged to a power source.

An interesting consumer application is bike fleet management. It consists in a fleet

of bicycles deployed around the city which can be used by people provided they subscribed some sort of agreement. The bicycles are usually locked, when the user pays to use them they are unlocked remotely and then a GPS module keeps track of its current position and finally records its destination to let another user find it on a map. The refresh rate should be quite frequent, up to 192 times per day. The devices are usually deployed outdoor, mostly because GPS would not be able to work indoor, but using different positioning technologies it could be interesting to have them working also indoor. It is estimated, according to [6], that up to 200 bikes per square kilometer could be present in an urban scenario. A similar use case is "pay as you drive", where a fleet of cars can be utilised by citizens. Cars can be also parked in indoor or underground parking areas, therefore the link budget should be capable of providing coverage also in this situations, provided that a localization technique, able to work indoor, is used. It is estimated that 2250 cars per square kilometer will be equipped with this technology.

Vending machines is another applications which will get benefits from LPWAN technologies. The transceiver will be used both to report periodically the amount of goods present inside, in order to plan efficiently the refill performed by the operators, but also to perform the payment through credit card. The number of packets transmitted in the latter case depend on the average number of people performing a transaction, which could be around 100 per day. To report on the current status is sufficient to perform one transmission per day with the summary of the whole day. The devices may be placed indoor and plugged to a power source, it is also expected to have around 150 vending machines per square kilometer.

IoT it is expected to bring great benefits also in the health care. We already have devices which can improve ill people's quality of life such as pacemakers or glucose monitors. These devices could be connected directly to the internet through LPWAN technologies. Apart from monitoring the health of the patient, they could also raise alarms in case a dangerous value of some variables is detected. A system of this kind should be very reliable and, even through the normal traffic pattern could be sparse, in case of emergency the packet should be delivered with low latency.

Finally another application involving localization is Very Important Person (VIP) or pet tracking. Similarly to the other aforementioned use cases, it is possible to equip pets or people with localization devices in order to be always aware on their position in case they are not able to return back home. The devices should be able to work indoor and they should update the current position quite frequently once the VIP or pet is declared lost by the user.

2.4 Use Cases Grouping

How to subdivide in macro groups the long list of use cases is a problem already addressed by others.

In [5] the authors assigned to each entry of their list of scenarios some grades considering certain performance metrics (battery life, mobility, security level and latency). Based on this grading system, four families were defined, from the most demanding applications to the least ones. For each case, the family is assigned following the following criteria:

- Type 1: high bandwith, mid latency, relatively short battery life, high mobility, high security
- Type 2: mid to high latency, long battery life, stationary, high security
- Type 3: medium battery life
- Type 4: powered, stationary, high-security

In Table 2.5 it is shown how some use cases were evaluated and assigned to each family in [5].

In [14] another criterion was applied and only two families were defined:

- Category 1: track, command, control & route, meaning the extension of the way of interaction between humans, machines, vehicles and nature.

Application Type	LPWA applications	Battery life	Mobility	Security	Latency
Type 3	Water metering	++++	+++	+++	+++
Type 3	Gas metering	++++	+++	+++	+++
Type 2	Microgeneration	+++	+++	+++	+
Type 3	Smart parking	++	+++	++	+++
Type 4	Smart Lighting	+	+++	++	+++
Type 3	Building Automation	++++	+++	+++	+
Type 1	VIP / Pet tracking	+	+	+++	++
Type 1	Smart bicycle	+	+	+++	++
Type 3	Industrial applications	++++	+++	+++	+++
Type 4	Vending Machines	+	+++	+++	++
...	...	...	...	...	...

Table 2.5: Use Cases grouping used in [5]

- Category 2: data mining, meaning all the applications that extract information from big data in order to provide specific services to users.

With such a large set of use cases we need a systematic method to analyze and provide performance evaluation for each of them.

The intention is to group all the possible use cases considering only non trivial differences which determine a specific environment and design of the system. In fact, some of the aforementioned metrics have an impact on the system design which are trivial and do not express the real capabilities of a technology, like the propagation environment or the network size that will affect only the deployment of the gateways/concentrators but not the capabilities of a single sink.

We already defined the performance metrics of our interest and in particular we mentioned how the offered traffic generated by the devices is expressed in packet per seconds because the sporadicalness of the traffic makes the actual amount of data generated by each device and the number of devices irrelevant. From the point of view of the sink the only relevant metrics are the total number of packets received per day and their size.

In other words, given a payload size, and so a packet duration, a single gateway or cell is able to process a certain number of packets per day approximately regardless of how many nodes are actually present in the network. This traffic, is the sum of the traffics generated by all devices in the network and the same amount of traffic

can be generated by a high number of devices which rarely transmit a packet or few devices which transmit packets at a higher pace. Based on this assumption, all the networks implementing use cases characterised by the same payload size will share the same ability to process their traffic.

We propose a grouping criterion based on this assumption, different use cases belong to the same group if they have the same payload size (P_L). In this way, we can perform simulations or other kinds of evaluations, on a representative use case for each group and extend the outcome of the evaluation to the other use cases.

We decided to define four groups based on the use cases described in section 2.3: Group A consists in all the use cases with $P_L \in [10, 20] B$, Group B with $P_L \in [20, 100]$ B, Group C with $P_L \in [100, 200]$ B, and finally Group D with $P_L = 1000$ B.

To prove the validity of this criterion, it is assumed to have a collision whenever two packets are overlapped in time, N nodes in the network, each of them producing λ packets per day, with a constant delay between two consecutive transmissions. Each packet has a duration, or Time on Air (T_A), which is a function of P_L. Assuming that a device starts transmitting with a uniformly distributed time offset, we can derive the following formula for P_s, given by Equation 2.5.

$$P_s = \left(1 - \frac{2T_A\lambda}{86400}\right)^{N-1} \tag{2.5}$$

Fig. 2.1 shows, as an example, P_s for six different use cases belonging to two different groups: Group B and Group C, when O is increasing. T_A has been determined assuming LoRaWAN is used. It is clear that use cases of the same group show a similar behavior in terms of success rate when the network traffic varies, which confirms the validity of our grouping criterion. When more complex protocols are employed by the devices, e.g. including retransmissions, the differences among the use cases of the same group tend to increase, but only marginally.

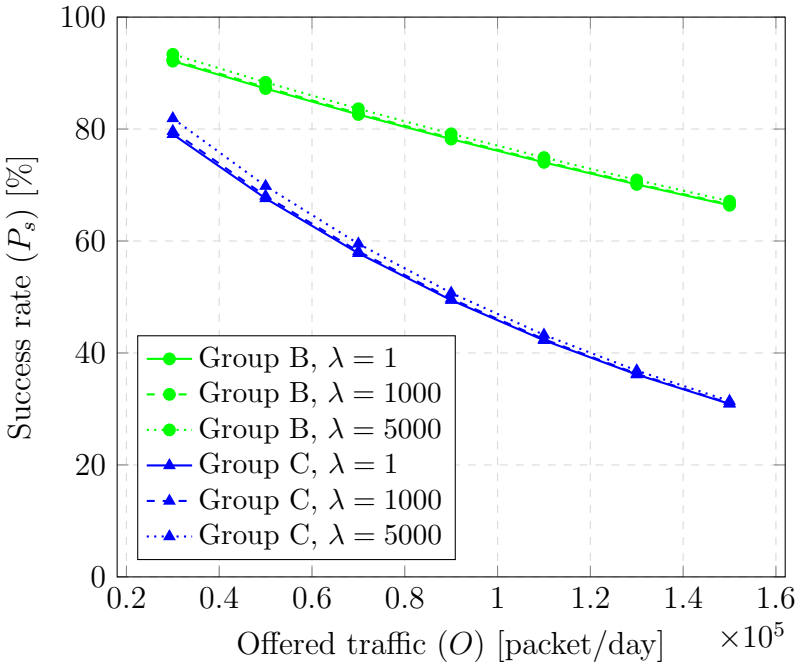

Fig. 2.1: Proof of concept for the grouping criterion

Category	**Use Case**	**Payload Size (P_L) [B]**	**Packet rate (λ) $\left[\frac{packet}{day}\right]$**	**Device density (ρ) $\left[\frac{devices}{km^2}\right]$**	**Coverage requirement**	**Battery requirement [years]**	**Maximum error rate ($P_{e,max}$)**	**Maximum Latency [s]**	**Group**
Consumer	Wearable	20	10	n.a.	Indoor	1	10 %	10	A
	White Goods	20	3	n.a.	Indoor	Powered	10 %	60	A
	Bike Fleet Management [6]	150	48	200	Outdoor	5	10 %	60	C
	Bike Fleet Management [5]	50	192	n.a.	Outdoor	5	10 %	60	B
	Pay as you drive	150	144	2250	Indoor	Powered	10 %	60	C
	Vending Machines [6]	150	1	150	Indoor	Powered	10 %	60	C
	Vending Machines [5]	1000	1	n.a.	Indoor	Powered	10 %	60	D
	Vending Machines Payment	100	100	n.a.	Indoor	Powered	10 %	10	C
	Assisted Living / Medical	100	8	n.a.	Deep Indoor	5	1 %	1	C
	VIP/Pet tracking	50	48	n.a.	Indoor	5	10 %	60	B
Industry 4.0	Asset Tracking	50	100	n.a.	Outdoor / Indoor	10	10 %	30	B
	Machinery Control	50	100	n.a.	Indoor	Powered	10 %	10 / 0.01	B
	Tank / Safety Monitoring	100	2	n.a.	Outdoor	10	1 %	60 / 1	C
Environmental Monitoring	Smart Agriculture	100	4	n.a.	Outdoor	10	10 %	60	C
	Animal Tracking	50	100	n.a.	Outdoor / Remote	5	10 %	60	B
	Data Collection	200	24	n.a.	Outdoor / Remote	10	10 %	60	C
	Events Monitoring	50	5	n.a.	Outdoor / Remote	10	1 %	1	B
Smart Buildings	Microgeneration	100	2	n.a.	Outdoor	Powered	10 %	60	C
	Home Automation	50	5	n.a.	(Deep) Indoor	Powered	10 %	60 / 0.1	B
	Smoke Detectors	20	2	n.a.	(Deep) Indoor	Powered	1 %	1	A
Smart Cities	Electricity Meters	100	1	10000	Indoor	10	10 %	60	C
	Gas Meters [6]	100	48	10000	Indoor	5	10 %	60	C
	Water Meters [6]	100	2	10000	Indoor	10	10 %	60	C
	Gas/Water Meters [5]	200	8	n.a.	Deep Indoor	10	10 %	60	C
	Smart Parking	50	60	3000	Indoor	5	10 %	60	B
	Waste Management	10	24	n.a.	Outdoor	10	10 %	60	A
	Lighting	100	5	n.a.	Outdoor	Powered	10 %	60	C
	Smart Grid	20	10	n.a.	Outdoor	10	1 %	1	A

Table 2.6: Use cases related to LPWAN and their requirements. [5, 6, 7].

Chapter 3

LoRaWAN

3.1 Introduction

LoRaWAN is one of the first technologies defined for LPWAN applications. Its standardization was initiated by Semtech, an American company which owns the patent for the synthesiser used to generate the modulated signal, and later by the LoRa Alliance, an organization of many companies which shared the effort to define a new standard for these new applications. Now, devices employing LoRaWAN are already in the market, and many organizations are starting using them to design their own IoT projects. Its simple access protocol is designed to avoid complexity and costs and to minimise the energy consumption while maximizing the transmission range. At the same time, the proprietary modulation used is very robust with respect to the interferers present in the shared bands used. Probably one of the most important aspects which boosted the commercial use of this technology, is the use of unlicensed band, which let anybody build their own system without the burden of subscribing to the licensed cellular bands.

The scientific literature on LoRa, and LPWANs in general, is expanding but at the time of these considerations most of the papers were only related to the link-level evaluation of the technology. Tests using Sigfox, LoRaWAN, and pre-standard NB-IoT solutions, have been made on the field by several network operators. Some field trials have been carried out, to determine LoRa ranging performance, in free space conditions [15] and in more complex scenarios [16].

Different studies have investigated the use of LoRa technology in specific fields of application, as for example, sailing monitoring systems [17], tactical troops tracking

systems [18], smart cities [19], etc. In contrast with these works, this thesis addresses a large set of applications, properly categorizing them.

Many details regarding the LoRa modulation and physical layer have been recently published in [20] and [21], where the Authors studied the output signal generated by commercial transceivers to understand how information is encoded and embedded in the chirp waveform.

The interference problem has been addressed in [22], where the Authors study packet collisions applying a time offset between each other; in [23] and [9] the orthogonality of transmissions performed with different Spreading Factors (SFs), an important issue discussed in more detail in section 3.3, is studied mathematically. More precisely, in these articles the Authors analyze the architecture of the LoRa (de)modulator and determine the conditions for a capture to happen in the presence of two signals with different SF. A similar analysis was performed, but using an experimental approach.

The first papers about the system-level LoRa network capacity have been published very recently, most of them addressing the problem through simple mathematical approaches [24, 25]. In these works the limitations imposed by regulation on the utilization of the channel are taken into consideration as a major limit for the network capacity; although this is true when few continuously transmitting devices are considered, if the traffic generated is more sporadic and the number of devices is higher, this does not represent a problem. It is possible to show that among the use cases considered in this thesis the channel utilization for a single device is always below 0.55%. Moreover, with respect to [24] and [25], I determine the capacity of a network considering the full LoRa protocol stack, the presence of concurrent transmissions and consequent collisions or captures, and realistic information on the physical layer obtained through experiments.

In [26] the Authors estimated, through simulations, the capacity of a LoRa network assuming a simpler collision mechanism and protocol than what was used in this work; these assumptions lead to a lower capacity.

In [27] the Authors studied experimentally the impact on the coverage of having multiple gateways deployed in a particular area of Glasgow. This thesis, though, focuses more on capacity than on coverage: a fact of relevance for LoRa, whose receive sensitivity depends on transmission parameters (the Data Rate (DR), defined more in detail in Section 4.2).

In section 4.2 the main aspects of the LoRaWAN technology are presented. In section 3.3 the LoRa technology is assessed through a set of experimental laboratory and on-field tests, to characterise it from the link-level viewpoint. The information gathered during these experiments, in terms of ranging capabilities and interference resilience, is used in section 3.5 to discuss the design and performance of a network deployed, first, in a small area employing a single gateway, and then in a larger area.

3.2 Technology

3.2.1 PHY Layer

LoRaWAN uses a proprietary modulation based on chirp spread spectrum, which exploits pulses whose frequency increases or decreases linearly over a certain amount of time; information is inserted in these pulses by introducing a discontinuity at different time offsets from the beginning of a symbol. These pulses occupy a Bandwidth (BW) which can typically take values of 125, 250 or 500 kHz. Interference problems are mitigated by employing forward error correcting codes in combination with frequency hopping spread spectrum. Fig. 3.1 shows a measurement of a transmission performed with the LoRa modulation. For the simulations performed in this thesis, I considered a network using three 125 kHz bands, from 868 MHz to 868.6 MHz, corresponding to the EU868-870 sub-band G1.

One of the most important parameters affecting the performance at physical level is the SF, that is, the ratio between the signal bandwidth and the symbol rate. Keeping the bandwidth constant, it is possible to enhance the receiver sensitivity

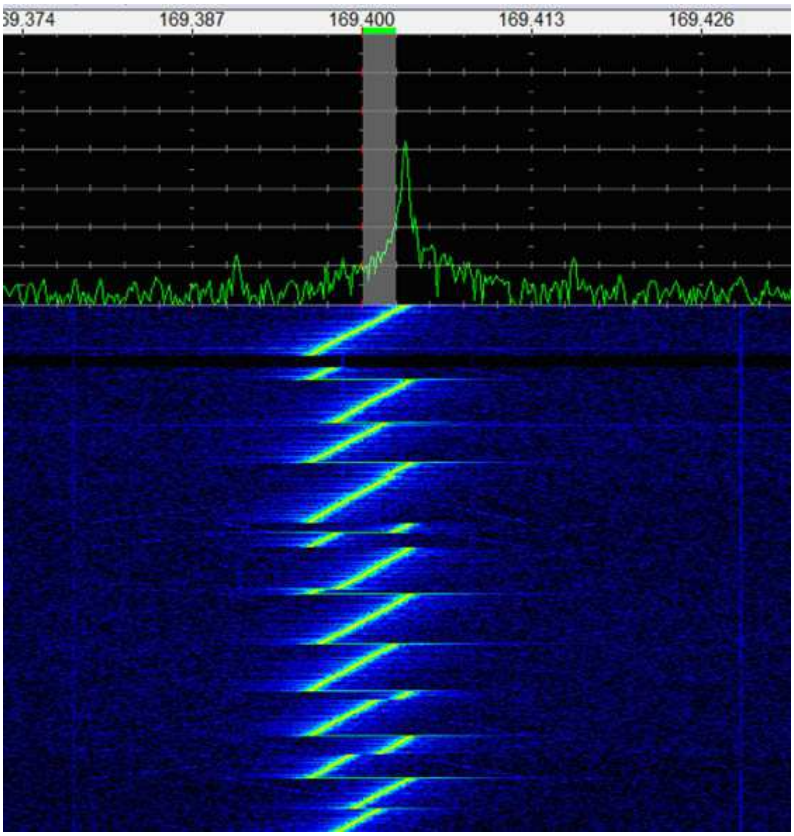

Fig. 3.1: Time-frequency representation of a LoRa transmission. [1]

by increasing the time on air (duration of a packet transmission). More precisely, each increment of the SF by one unit, from the minimum value 6 to the maximum value 12, corresponds to a doubling of the time on air and a decrement of the receiver sensitivity of roughly three dB. As a reference case, with BW=125 kHz, the receiver sensitivity at the End Device (ED) is -125 dBm and -137 dBm, for SF=7 and 12, respectively. Transmissions with different SFs are claimed to be orthogonal.

The documentation refers often to the DR rather than the SF directly. In the LoRaWAN documentation framework, each DR value corresponds to a specific combination of SF and BW. This correspondence, defined in the LoRa Specifications [28], is reported in Table 3.1. It is clear that, for most of the possible settings, an increment of the DR directly corresponds to a decrement of the SF [29, 30].

DR	Configuration	Indicative physical bit rate [bit/s]
DR0	SF12 / 125 kHz	250
DR1	SF11 / 125 kHz	440
DR2	SF10 / 125 kHz	980
DR3	SF9 / 125 kHz	1760
DR4	SF8 / 125 kHz	3125
DR5	SF7 / 125 kHz	5470
DR6	SF7 / 250 kHz	11000

Table 3.1: Datarate definition for EU863-870.

3.2.2 MAC Layer

The LoRaWAN MAC describes three Classes: i) Class A: EDs, after the transmission of a packet, open two receive windows to get an Acknowledgement (ACK) or receive data from the Gateway (GW), then they stay in idle mode until the next transmission; ii) Class B: EDs have more receive windows synchronised with a beacon provided by the GW; iii) Class C: EDs continuously stay in reception mode and a downlink message may be received at any time.

LoRaWAN networks form a star topology rooted at a LoRaWAN GW, and any device has to be compliant with, at least, Class A (considered in this thesis), where in uplink ALOHA protocol is used or, in other words, the transmission may be initiated at any time with a certain probability of collision with other transmissions. There are two types of transmission mode: confirmed, using ACKs, and unconfirmed, when no ACKs are used. When an ACK is expected but not received by the transmitter, a recovery algorithm, which consists in multiple retransmissions, is initiated. The maximum number of retransmissions suggested in the specification is eight. The standard does not specify any other detail regarding the settings to use for the retransmission. When the simulations described afterwards were performed, the specification suggested to decrement the DR every two failed retransmissions. Nevertheless, in later revisions the LoRa Alliance removed this indication. With the strategy considered the SF increases and the time on air increases as well. This algorithm implicitly assumes that the transmission failed due to poor connectivity, therefore a lower DR should increment the success rate, as the receiver sensitivity

will be better.

3.3 Link Performance

We performed two types of link-level assessment via experimentation, both needed to properly capture the link performance in system-level simulations. First, I measured the received power as a function of distance; then I assessed the claimed orthogonality of transmissions made with different SFs, and the protection ratio when the same SF is used by two simultaneously transmitting devices.

3.3.1 Experimental Setup

In order to characterise the transmission range of a LoRa device we performed measurements of received power at increasing distances, with the aim to define a path loss model usable also in different conditions. Two Semtech SX1272 modules were used during this experiment, one deployed on a 240 m high hill and the other one, the transmitter, deployed in different locations at increasing distances in flat terrain (Fig. 3.2). The maximum distance reached in this experiment was 10,8 km and for each location LoS conditions were met. The Received Signal Strength Indicator (RSSI) provided by the transceiver was used as a measurement of received power after being averaged over the transmission of 10,000 packets per location. The devices were configured to transmit using BW=250 kHz, coding rate 4/5, packets with a 18 byte payload and a transmit power P_t= 14 dBm. Measurements are discussed in sub-section 3.3.2.

In order to check the orthogonality among transmissions with different SFs, a wired testbed was setup using Semtech SX1272 as a receiver, and two Microchip RN2483 transceivers as transmitters. The experiments were conducted in a laboratory inspired to the methodology described in [31]. The two sources transmitted packets starting simultaneously, containing independent payload and using different SF. The signal resulting from the mixing of the two transmitters outputs, is being du-

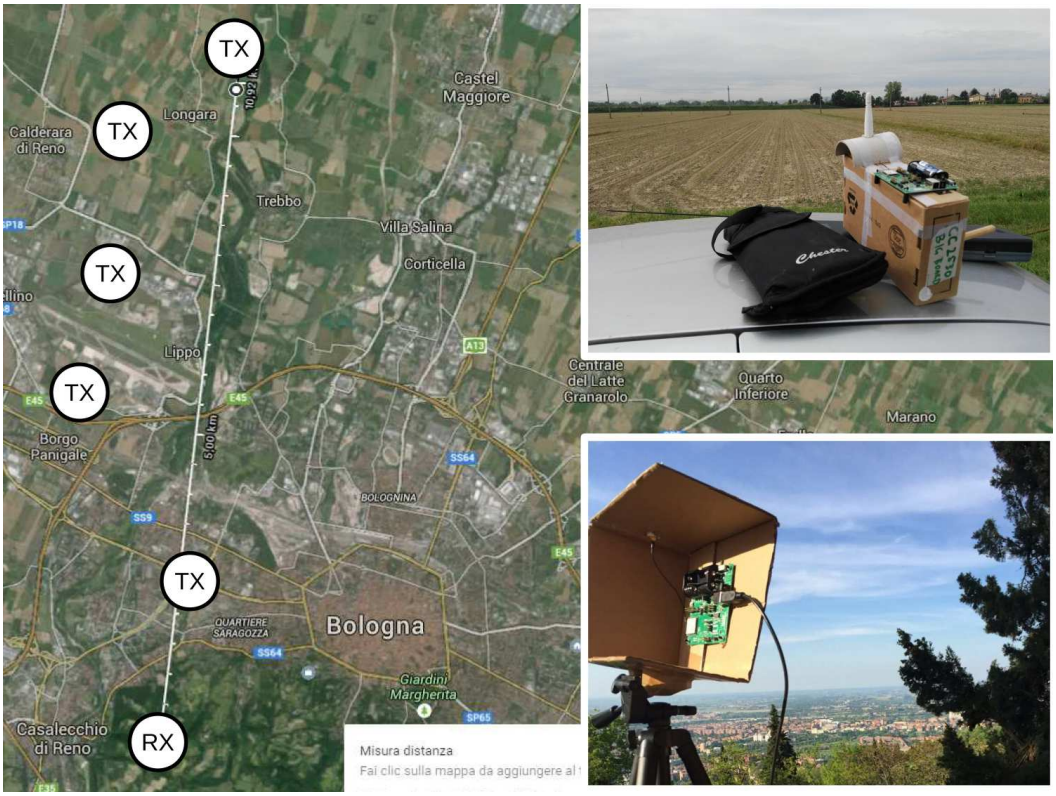

Fig. 3.2: Map of Bologna: setup for ranging experiments with fixed gateway.

plicated, sent to the receiver and to a spectrum analyzer which is used to measure the Signal-to-Interference Ratio (SIR), defined as the ratio between the peak power of the intended received signal, and the peak power of the interfering signal. For each level of SIR, 10,000 packets were transmitted and the number of captured (i.e., correctly received) packets were counted, to assess the packet success rate (P_s). From the resulting curve, the protection ratio (α) is derived as the value of SIR which implies a success rate of 50%.

The protection ratios found according to this methodology are representative only of a situation where no time offset is present between two colliding packets. Nevertheless it is expected that the presence of a time offset would reduce the overlap between the two packets and ultimately the amount of energy causing a collision. Therefore the results presented in this work can be considered as a worst case.

Measurement results are described in sub-section 3.3.3.

3.3.2 Transmission Range

Fig. 3.3 presents the results of the measurements focused on the ranging capabilities of LoRa. Three dashed curves, one for each SF considered, show how the RSSI decreases as the distance increases; the SFs were chosen from the set $\{7, 9, 12\}$.

In Fig. 3.3 it is shown also the expected received power according to the Okumura-Hata model, as described in section 2.1, when the same scenario is considered and in absence of antenna gains and cable losses.

We observed an almost constant difference between the "Okumura-Hata" curve and our measurements: a gap of about 27 dB, which may be caused by antenna mismatches and other technological impairments. Assuming that this additional loss is present whenever the LoRa technology is involved, in order to use the model as defined in section 2.1 and (2.2), we consider from now on $G_{tot} = -27dB$.

Finally, in Fig. 3.3 the curve "Channel Model" represents the resulting received power according to (2.2) after the estimation of G_{tot}. The values for the other parameters are reported in Table 2.1 whereas P_t=14 dBm; therefore P_{r0}= -99.2 dBm.

3.3.3 Orthogonality of Spreading Factors

The SFs used by the devices were chosen in the set $\{7, 9, 12\}$. A first measurement campaign was conducted, letting the two transmitters use the same SF. In this case the lack of orthogonality brings to packet losses, as long as the SIR is not sufficiently large. Only minor differences were found when varying the SF. Defining conventionally the protection ratio, α, as the value of SIR that ensures a success rate equal to 50%, I then found it varies from 0.3 dB to 1.7 dB (see 3.2).

A second campaign was conducted to study the assumption of orthogonality among transmissions performed using different SFs. In Table 3.2 it is reported the estimated protection ratios in dB for all the cases already mentioned. As expected, the impact of the interferer on the useful transmissions is much smaller, but in any case

		Useful Signal		
		SF7	SF9	SF12
Interfering Signal	SF7	0.3	-10.3	-11
	SF9	-13.8	0.3	-14.6
	SF12	< -30	-21.6	1.7

Table 3.2: LoRa Protection Ratios in dB.

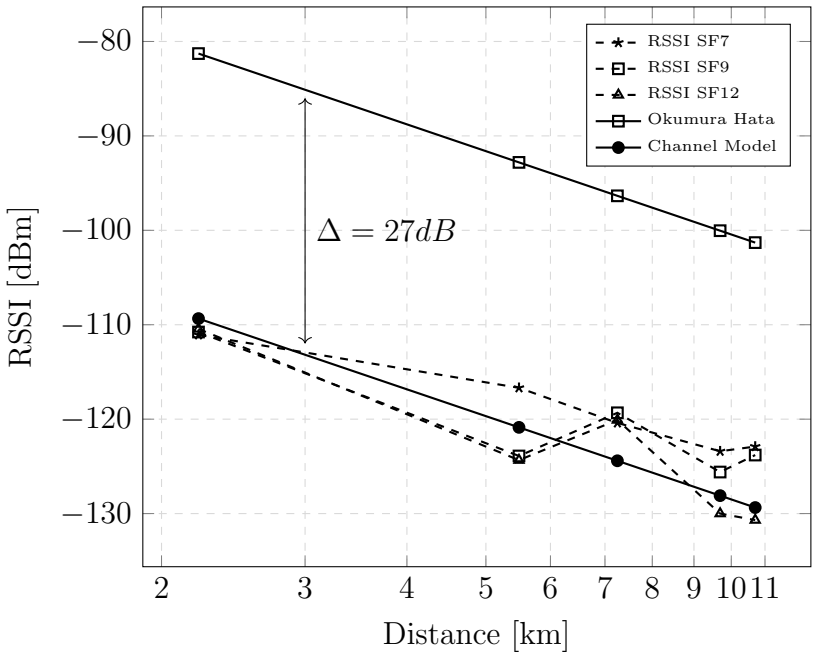

Fig. 3.3: Measured average RSSI [dBm] as a function of distance [km] and comparison with Okumura-Hata model.

different SFs are not perfectly orthogonal.

The effect of this lack of orthogonality may have an impact when a large network is considered; for example, in a network where all devices use the same transmit power, an interferer which is from 2 to 5 times closer to the gateway than another device, may cause a collision even when a different SF is used.

In the literature the possibility to have virtual orthogonal sub-channels is often mentioned, but some of the devices working in a given sub-channel will always be potential interferers for another set of devices working in a different sub-channel,

depending on their relative positions. However, this phenomenon can be considered as a second order effect since collisions due to the random access within the same sub-channel have a much stronger impact.

3.4 LPWAN Simulator

A system-level simulator was built accounting for the main features of LoRaWAN MAC and the link-level aspects discussed above.

Initially, the simulator was designed to support multiple technologies and protocols, thus it consists of several components managing different aspects of the simulation. As depicted in Fig. 3.4, the component *GEOMETRY* manages the deployment of the devices in a three-dimensional environment. From a configuration file it is possible to indicate how many devices should be deployed uniformly in a certain area or volume; this component, then, generates a series of files containing the positions of all the devices in a set of scenarios. This components provides also indication to the simulator on how to compute the path loss, according to (2.1). The channel parameters are specified in the configuration file. Similarly, the component *TRAFFIC* generates a series of events representing the transmission requests of the application for each node for the entire duration of the simulation. These components manage all the aspects of the simulation that are not related to the technology used.

The *SIMULATOR CORE* executes the simulations based on the scenario description provided, it is divided in a technology dependent component implementing the most important features of the technology considered, in this case LoRaWAN, while the *Channel Model* component computes the received powers of each transmission determining if they were successful or not.

Finally the *Post Processing* component collects both the input and outputs of the simulations and computes the metrics of interest by comparing them, again, regardless of the technology used. If multiple scenarios are generated, these metrics are the average among them.

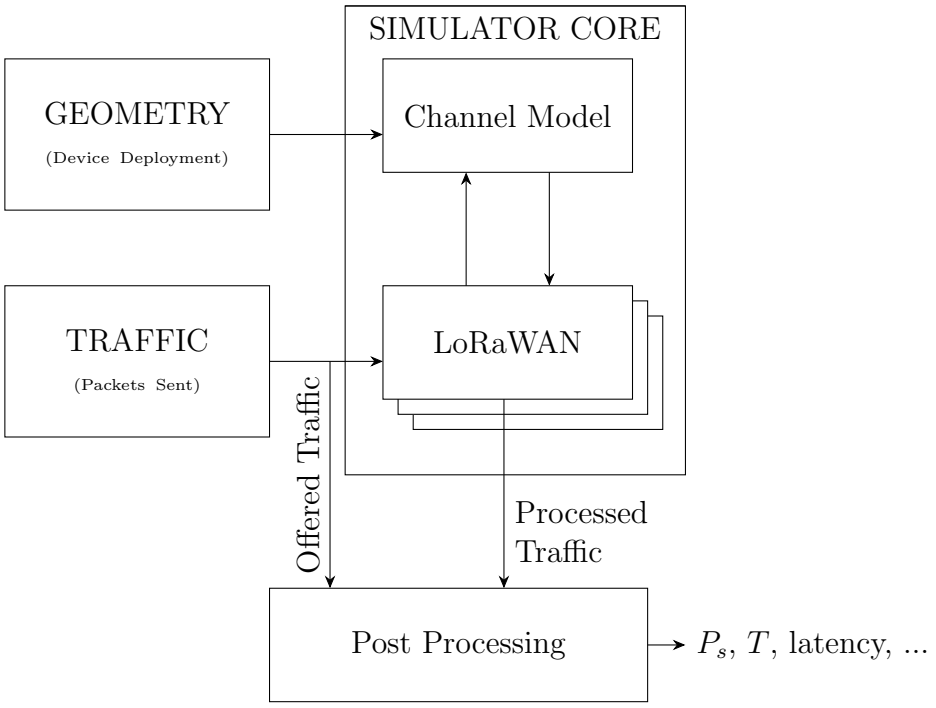

Fig. 3.4: Architecture of the LoRaWAN Simulator.

Due to the asynchronous nature of LoRaWAN, the simulator was developed as event driven. The underlaying software architecture supports multiples entities generating events which are then processed in sequential order.

In order to simplify and organise the code, each device consists of three entities implementing different aspects of the protocol, from the PHY to the upper layers. Being a commercial GW able to receive multiple packets at the same time, its simulated version is composed by multiple instances of the entities managing the reception of packets with a specific configuration. Fig. 3.5 represents the aforementioned structure and it shows the exchange of events among all the entities during an uplink transmission.

Regarding the simulations performed in the following sections, I assume the area to cover is a square of area A_{sim}, where N sensors are deployed randomly and uniformly. We also account for log-normal shadowing with standard deviation σ_S, a coherence time $T_C = 200\ s$, and a negative exponential autocorrelation function [32], while the path loss is calculated according to section 2.1 and considering the

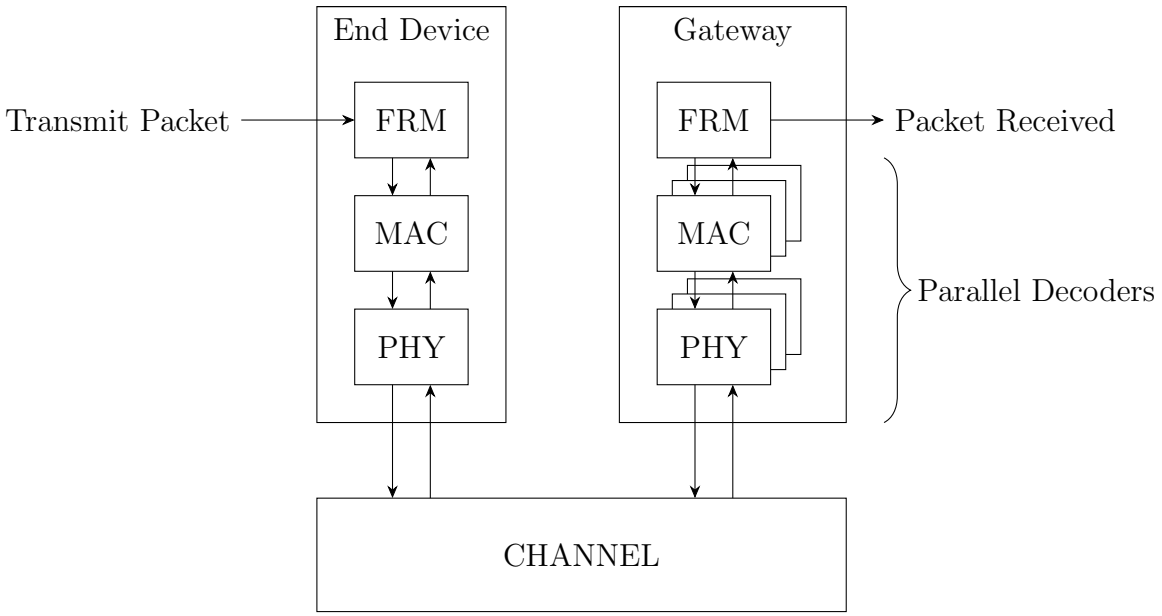

Fig. 3.5: Detail of event exchange in LoRaWAN simulator.

GWs to be placed at a height of 30 m from the ground. As already mentioned in section 3.3.2 the different height has an impact on the path loss formula. For the simulations the path loss parameters which will be used are reported in Table 2.1 as "Okumura-Hata rural".

Different scenarios characterised by a different number of gateways are considered. When multiple gateways are deployed they may receive multiple replicas of the same packet; in that case only one reception is considered in the final statistics.

The nodes wake-up, sample and transmit their data through the LoRaWAN access mechanism at regular time intervals in such a way that each of them generates λ packets per day. The global offered traffic is $O{=}N\lambda$.

A packet is detected by a device if the received power is greater than the sensitivity; if this happens the device will lock to the preamble and will try to decode the payload. When a collision between more packets happens, with any time offset, their SIR is calculated and the payload is passed to the upper layers if the device is locked to that particular packet and if the SIR is greater than α as estimated in section 3.3.3.

To emphasise the role of proper link-level considerations, I used the simulator to compute the curves previously shown in Fig. 2.1. The resulting curves are closer to a more realistic value with an absolute difference from the theoretical ones between 20% and 40%.

The most important simulation outputs consist in P_s, calculated as the ratio between the number of packets correctly received by the network and those transmitted by the devices, and the network throughput, T, calculated as the quantity of information correctly received by the network per unit of time (see (2.3)).

Network capacity will be defined later based on discussions about the relationship between P_s, T and the offered traffic O. This will also require the identification of the best transmission mode (initial SF, confirmed or unconfirmed) for each use case/scenario considered.

3.5 System Performance Estimation

3.5.1 Capacity of a Small Area

The purpose of this section is to estimate the capabilities of one, or more, gateways in different scenario and for different applications. Due to the large variety of use cases mentioned in section 2.3, I exploit the considerations described in section 2.4 and one representative use case for each group was chosen. These use cases are Waste Management in Smart cities for Group A, Animal Tracking for Precision Agriculture for Group B and Environmental Data Collection for Group C (see Table 2.6 for further details).

We considered a scenario consisting in a square area of $A_{sim} = 1\ km^2$ where a variable number of nodes is deployed and a LoRa gateway, placed in the center, is sufficient to cover all of them using any SF. For each group of use cases I vary the number of nodes to simulate different amounts of offered traffic. Let us define the network capacity as the amount of offered traffic which allows to maximise the network throughput. In Fig. 3.6 I report four curves representing how the

network throughput varies as the number of devices, and therefore the offered traffic, increases. Each curve represents a different configuration of the PHY and MAC parameters: confirmed or unconfirmed mode and initial SF equal to 7 or 12. In case of retransmissions, the SF increases as mentioned in section 4.2. For the sake of simplicity I only show the results for the use cases of Group B.

It is evident that initial SF equal to 7 and unconfirmed mode is the configuration that allows the highest throughput which, for Group B, is around 300 B/s when the offered traffic is 1.3×10^6 packet/day. This is because of the small area size.

The problem with this definition of capacity, though, is that it leads to an operating point where the packet success rate is around 39% for the case of Group B, which is too low for many applications. The same happens also for the other groups. For this reason I redefine the network capacity, O_{max}, as the maximum amount of offered traffic O which guarantees a maximum level of packet error rate $P_{e,max}$.

Figures 3.7, 3.8 and 3.9 show how the packet success rate changes when the offered traffic increases for the three groups and for each different configuration used.

Generally speaking, in case of a small area to cover, the best solution is to set the SF to 7 in order to avoid collisions by keeping the packet time on air, and so the SF, as small as possible. Moreover, when there is not much traffic in the network, the confirmed mode is the best choice to guarantee a high success rate.

When the network is more congested, the chosen retransmission mechanism increases the collision probability which leads to a lower success rate and throughput; for this reason the curves for SF7 and confirmed mode become lower than the curves for SF7 and unconfirmed mode when the offered traffic becomes higher than a certain value. This can be observed easily in Figures 3.7 and 3.8, while in Fig. 3.9 this phenomena happens at higher amounts of offered traffic.

From these curves, considering the desired maximum error rates reported in Table 2.6, I derived the network capacity for the different use case groups; this capacity is always reached when confirmed mode and SF7 are used. All the resulting capacities are reported in Table 3.3. For each use case the network size, or the maximum

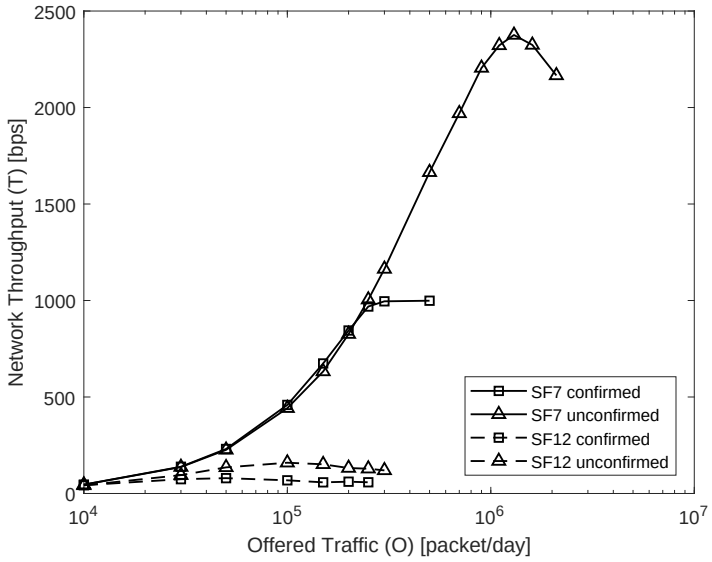

Fig. 3.6: Simulations: network throughput for Group B ($P_L = 50B$, $\lambda = 100$ packet/day).

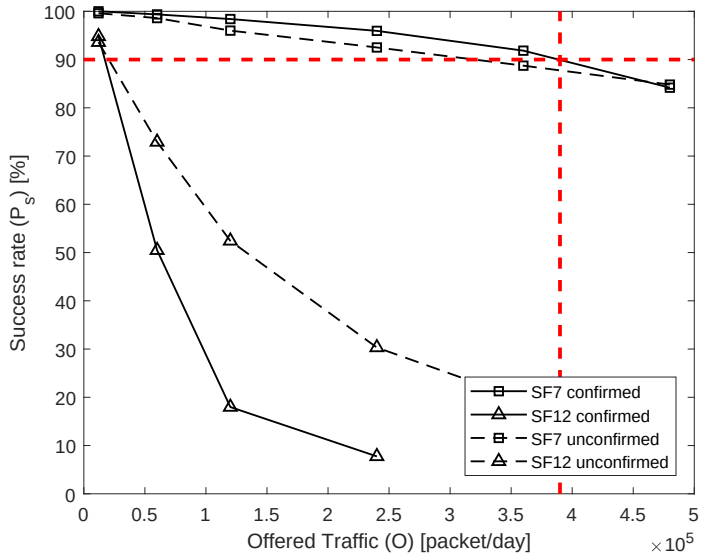

Fig. 3.7: Simulations: success rate for Group A ($P_L = 10B$, $\lambda = 24$ packet/day).

number of devices that guarantees the required success rate, can be calculated as N_{max}=O_{max}/λ. Moreover, the maximum node density compatible with the requirement is given by ρ_{max} =N_{max}/A_{sim}. These results are shown in Table 3.3

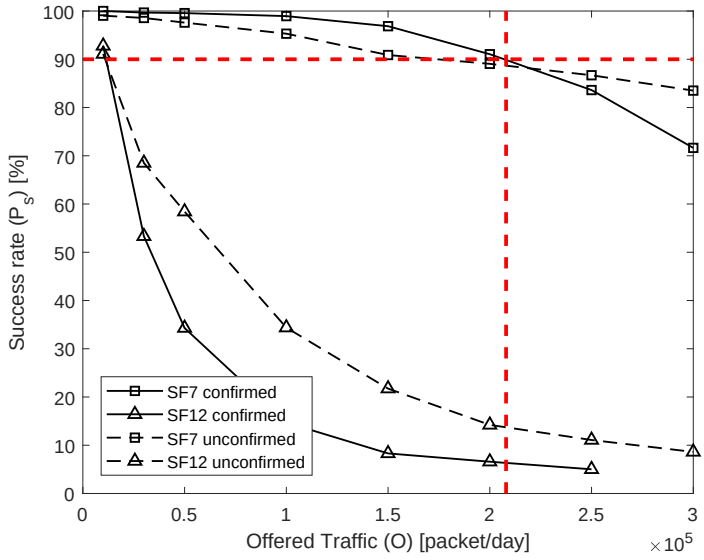

Fig. 3.8: Simulations: success rate for Group B ($P_L = 50B$, $\lambda = 100$ packet/day).

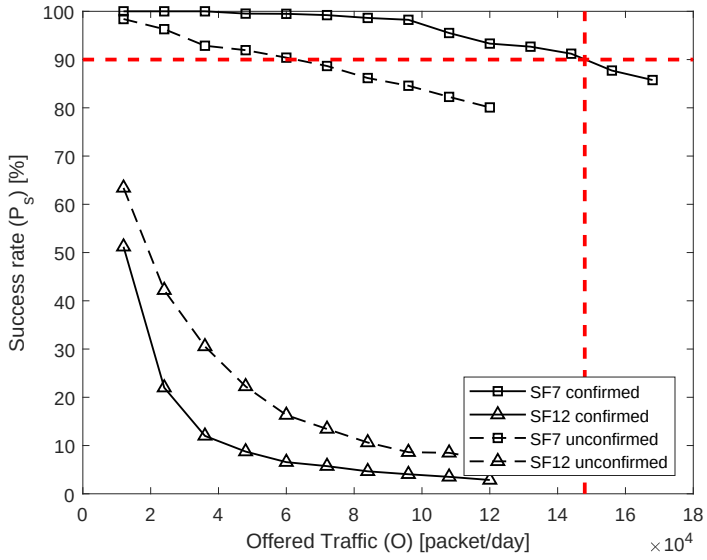

Fig. 3.9: Simulations: success rate for Group C ($P_L = 200B$, $\lambda = 24$ packet/day).

as well.

It can be noticed, by comparing the column "N_{max}" with the number of devices that would be present in the aforementioned scenario considering the densities specified

in Table 2.6, that in some cases a single GW is not sufficient to satisfy all the users deployed. These use cases are “Pay as you drive”, “Asset Tracking” and “Gas Meters”.

The average latency, defined as the average delay between the request of transmission at device side and the notification to the application layer of correct reception at gateway side, is 4.1, 6.9 and 7.8 seconds for Groups A, B and C, respectively. This high latency is due to the retransmission mechanism employed to achieve the higher capacity, but it can be easily reduced below one second by using unconfirmed mode which cause a drop in the success rate of less than 10%.

3.5.2 Coverage of a Large Area

Let us assume to have a scenario where the area to cover is larger. As already discussed, a solution to the problem may be to increase the SF used by the devices; in this way the transmission range of the devices is larger but the radio channel is utilised more intensively due to longer packet durations, a behavior that can lead quickly to the saturation of the network. Another solution is to deploy more gateways in the territory; this allows us both, to cover a larger area without the need for the devices to use a high SF, and also to keep the channel utilisation low avoiding network congestion.

According to the LoRaWAN specification, when a device sends a packet, potentially all gateways in the network could receive it. It is sufficient that only one is received to succeed. This implies that the higher is the amount of gateways in the networks, the higher is the success rate.

Before analyzing the network capacity, a set of simulations have been performed to study the benefits of having multiple gateways; the scenario considered is a square area of side 6.82 km ($A_{sim} = 46.5\ km^2$), which is represented in Fig. 3.10; the gateways are disposed in a hexagonal grid and every cell has a radius R_{cell}= 1.97 km which corresponds to the average transmission range of a LoRa device considering the downlink, SF7 and the channel path loss formula already used in

Category	**Use Case**	**Payload Size (P_L) [B]**	**Packet rate (λ) [$\frac{packet}{day}$]**	**Maximum error rate ($P_{e,max}$)**	**Group**	**Network Capacity (O_{max}) $\times 10^3$ [$packet/day$]**	**Network Size (N_{max}) $\times 10^3$ [$devices$]**	**Node Density (ρ_{max}) [$devices/hectare$]**
Consumer	Wearable	20	10	10 %	A	390	39	390
	White Goods	20	3	10 %	A	390	130	1300
	Bike Fleet Management [6]	150	48	10 %	C	148	3.08	30.8
	Bike Fleet Management [5]	50	192	10 %	B	208	1.08	10.8
	Pay as you drive	150	144	10 %	C	148	1.03	10.3
	Vending Machines [6]	150	1	10 %	C	148	148	1480
	Vending Machines [5]	1000	1	10 %	D	n.a.	n.a.	n.a.
	Vending Machines Payment	100	100	10 %	C	148	1.48	14.8
	Assisted Living / Medical	100	8	1 %	C	75	9.38	93.8
	VIP/Pet tracking	50	48	10 %	B	208	4.33	43.3
Industry 4.0	Asset Tracking	50	100	10 %	B	208	2.08	20.8
	Machinery Control	50	100	10 %	B	208	2.08	20.8
	Tank / Safety Monitoring	100	2	1 %	C	75	37.5	375
Environmental Monitoring	Smart Agriculture	100	4	10 %	C	148	37	370
	Animal Tracking	50	100	10 %	B	208	2.08	20.8
	Data Collection	200	24	10 %	C	148	6.17	61.7
	Events Monitoring	50	5	1 %	B	100	20	200
Smart Buildings	Microgeneration	100	2	10 %	C	148	74	740
	Home Automation	50	5	10 %	B	208	41.6	416
	Smoke Detectors	20	2	1 %	A	83	41.5	415
Smart Cities	Electricity Meters	100	1	10 %	C	148	148	1480
	Gas Meters [6]	100	48	10 %	C	148	3.08	30.8
	Water Meters [6]	100	2	10 %	C	148	74	740
	Gas/Water Meters [5]	200	8	10 %	C	148	18.5	185
	Smart Parking	50	60	10 %	B	208	3.47	34.7
	Waste Management	10	24	10 %	A	390	16.3	163
	Lighting	100	5	10 %	C	148	29.6	296
	Smart Grid	20	10	1 %	A	83	8.3	83

Table 3.3: Maximum capacity of a single LoRaWAN Gateway in a small area per Use Case.

the previous section. Simulations are performed by varying the number of sinks deployed, in particular a scenario with only gateway A is considered first, then a network with only four gateways (A, B, C and D), and finally one with all seven gateways deployed. Notice that when all gateways are considered the area is fully covered with SF7, while when only gateway A is present a SF higher than 10 is needed to cover the area. The devices in the network generate an offered traffic (O) of approximatively 112 thousands packet/day.

Fig. 3.11 shows how the success rate increases as the number of gateways employed rises. All the curves shown represent the performance of the network when unconfirmed mode is selected. The dashed curves are made considering initial SF= 7 while the solid ones considering initial SF= 12.

When the initial SF is 7 the network is not congested, therefore every packet is received by a gateway that is simply within the transmission range of the sender; in this case the improvement in terms of success rate, represented by the dashed lines, is given by a better geometrical coverage provided by the additional gateways. This can be seen also by comparing the three curves with the "Geometrical Coverage" curve, which represents the fraction of the area defined by the union of all the circles centered in the gateway locations and with radius equal to the transmission range with SF7, with respect to the total area. This curve is very close to those mentioned above, proving that all the effects related to the MAC protocol are negligible.

When the initial SF is 12, the geometrical coverage is always 100%, so the improvement represented with the solid lines is only due to the higher probability of having at least one packet received with a signal to interference ratio higher than the protection ratio. This improvement is similar among the three groups; their success rates differ only in the absolute value due to the different payload sizes which cause different levels of congestion when O is fixed, as in this case.

The previous statement can be confirmed also by observing the set of points representing the case with only one gateway deployed; this case differs from the one discussed in the previous section only in the size of the area. The success rates when the initial SF= 12 are identical in both scenarios, being the transmission

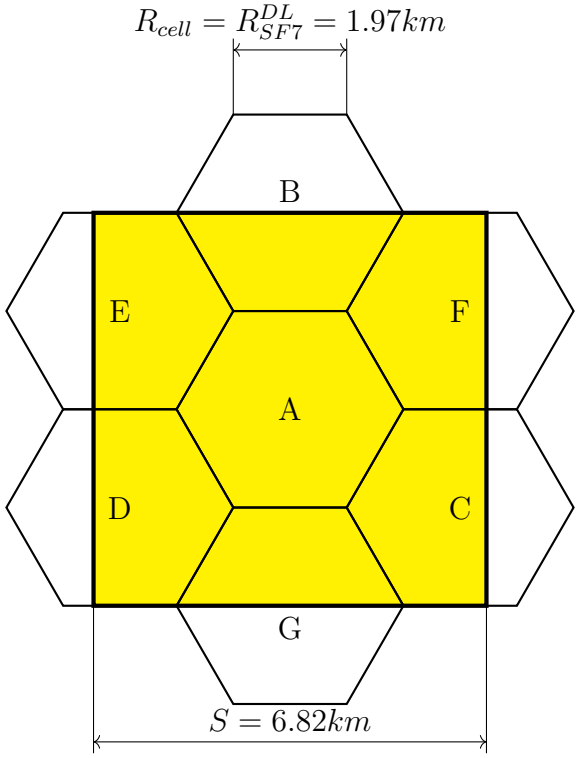

Fig. 3.10: Scenario with multiple gateways.

range enough to cover all the devices in both cases, while with initial SF= 7 the success rate values are close to the amount of area in range, 100% when the area is small, 55% when it is large.

It is evident that, for the scenario proposed, the option that guarantees the highest success rate, therefore network capacity, is to use seven gateways and SF7.

3.5.3 Capacity of a Large Area

We now move to the characterization of P_s versus O as done in section 3.5.1, this time varying the number of gateways in order to estimate how the network capacity improves when a more complex network is considered. For the sake of simplicity we consider only Group C and SF7. The four curves in Fig. 3.12 represent the behavior of the network when confirmed or unconfirmed mode is used and when the number of gateways varies from one to four.

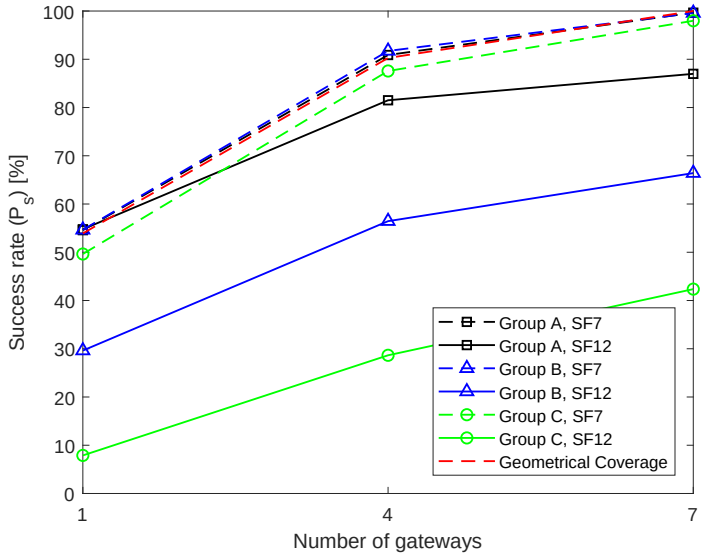

Fig. 3.11: Success rate for the three groups as a function of the number of gateways.

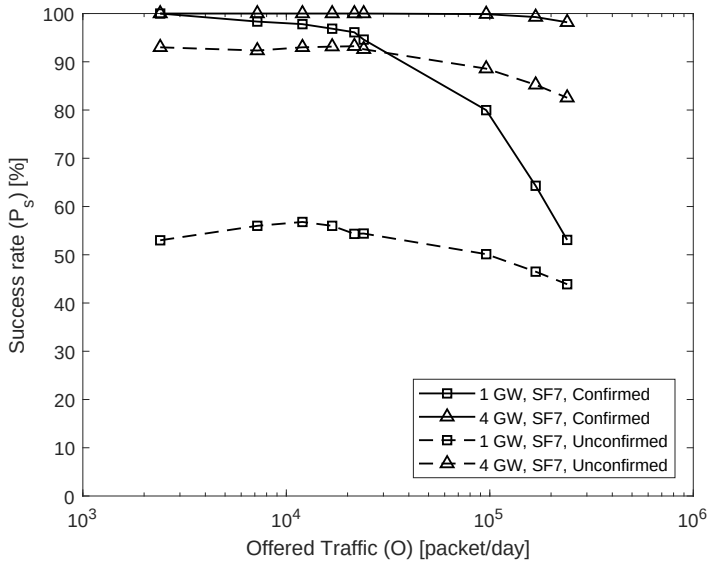

Fig. 3.12: Simulations: success rate for Group C with different number of Gateways ($P_L = 200B$, $\lambda = 24$ packet/day).

When unconfirmed mode is used, the amount of traffic has a minor impact on the success rate as the geometrical coverage plays the main role, resulting in a success rate of 55% or 93% depending on the number of gateways.

When confirmed mode is used the coverage problem is overcome, therefore the success rate is limited only by capacity issues. When only one gateway is present, the success rate requirement ($P_{e,max}$= 10%) is satisfied with an offered traffic smaller than O_{max}= 40 thousands packet/day, a significantly smaller value with respect to the scenario described in section 3.5.1 because more devices tend to use a higher SF in order to reach the gateway. When four gateways are present, the minimum success rate is reached with an offered traffic O_{max}= 1.5 million packet/day, much higher than the case with only one gateway.

In Table 3.4 it is reported the capacity (O_{max}), the size (N_{max}) and the maximum node density (ρ_{max}) of a network implementing the use cases of Group C.

It can be noticed, similarly to section 3.5.1, that comparing the maximum node density with the use case requirement, when only one GW is deployed, three Class C use cases cannot be satisfied ("Pay as you drive", "Gas Meter" and "Water/Gas Metering"). Nevertheless, when 4 GWs are considered they can all be satisfied.

Category	**Use Case**	**Network Capacity** (O_{max}) $\times 10^3$ $[packet/day]$	**Network Size** (N_{max}) $\times 10^3$ $[devices]$	**Node Density** (ρ_{max}) $[devices/hectare]$
1 Gateway				
Consumer	Bike Fleet Management [6]	40	0.83	1.8
	Pay as you drive	40	0.3	0.6
	Vending Machines [6]	40	40	86
	Vending Machines Payment	40	0.4	0.86
	Assisted Living / Medical	4.8	0.6	1.3
Industry 4.0	Tank / Safety Monitoring	4.8	2.4	5.2
Environmental Monitoring	Smart Agriculture	40	10	22
	Data Collection	40	1.7	3.6
Smart Buildings	Microgeneration	40	20	43
Smart Cities	Electricity Meters	40	40	86
	Gas Meters [6]	40	0.83	1.8
	Water Meters [6]	40	20	43
	Gas/Water Meters [5]	40	5	10.8
	Lighting	40	8	17
4 Gateways				
Consumer	Bike Fleet Management [6]	1500	31.3	67.2
	Pay as you drive	1500	10.4	22.4
	Vending Machines [6]	1500	1500	3226
	Vending Machines Payment	1500	15	32.3
	Assisted Living / Medical	190	23.8	51.1
Industry 4.0	Tank / Safety Monitoring	190	95	204
Environmental Monitoring	Smart Agriculture	1500	375	807
	Data Collection	1500	62.5	134
Smart Buildings	Microgeneration	1500	750	1613
Smart Cities	Electricity Meters	1500	1500	3226
	Gas Meters [6]	1500	31.3	67.2
	Water Meters [6]	1500	750	1613
	Gas/Water Meters [5]	1500	188	403
	Lighting	1500	300	646

Table 3.4: Network capacity for the use cases in group C in a large area.

Chapter 4

NB-IoT

4.1 Introduction

NB-IoT [33] is an access technology defined by 3GPP for mMTC. NB-IoT implements several mMTC-oriented enhancements compared to other mobile technologies [34, 35, 8]; examples are: *(i)* narrow-band transmission and the exploitation of repetitions to reach devices in challenging positions such as basements or underground; *(ii)* differentiation of User Equipement (UE) performance according to coverage areas by tuning parameters of the physical channels and network procedures; *(iii)* enhanced power saving mechanisms to improve the battery life; *(iv)* simplification of network procedures to reduce the UE complexity. In addition, being fully integrated within 3GPP networks, NB-IoT can be enhanced to support services usually delivered in mobile networks, as testified by the introduction of multicast capabilities in the recent updates of the standard [36]. Several works and white papers, e.g., [33, 37, 38, 39], present an overview of the main features of NB-IoT and study performance in terms of coverage extension or Random Access (RA) capacity. Information on NB-IoT are thus currently spread across several technical documents and publications, and an overall overview of all the different features of NB-IoT, is still missing.

The aim of this chapter is twofold. Firstly, a detailed overview of NB-IoT summarizing all main features and technical information is provided. This includes a presentation of NB-IoT from both Uplink (UL) and Downlink (DL) perspectives, motivated by the growing attention towards remote re-configuration of IoT devices. To this aim, the procedures for DL and Single Cell Point to Multipoint (SC-PTM)

transmissions are summarised, in addition to the UL case. We discuss in details the configuration capabilities of NB-IoT for parameters such as number of repetitions, physical channel configurations, timers, etc. We also present a detailed discussion of the main sources of latency in both UL and DL directions. Notably, I analyze how latency might vary according to the NB-IoT cell configuration. Above discussions are supported by a performance evaluation of UL and DL considering real mMTC use cases.

The second aim is to present a mathematical model able to predict the success probability, the fairness of service provided and the maximum throughput possible with a certain configuration of the design parameters in a given scenario. We further present an analysis on how these parameters affect the overall performance and how the optimal configuration in terms of coverage classes may be chosen according to arbitrary criteria.

Finally, another contribution of this paper is the analysis of a new use case, i.e., firmware update of a group of devices, conducted by comparing the performance achieved with DL (i.e., unicast) and SC-PTM transmission schemes.

The remainder of this chapter is organised as follows: Section 4.2 contains a detailed description of the NB-IoT standard and all the configuration parameters of importance, whereas Section 4.3 provides a description of the mathematical model of a NB-IoT network mentioned above. Finally, Sections 4.4 and 4.5 report respectively an estimation of the performance considering given use cases and both unicast and multicast communication, and a study on the degrees of freedom available to configure the network and some indications on how optimise the performance metrics of interest.

4.2 Technology Overview

4.2.1 Extended Coverage

NB-IoT targets a coverage improvement of 20 dB w.r.t. GSM/GPRS, achieved through the utilization of *narrow-band signals* and *time diversity*.

A narrow-band signal allows the receiver to filter out more noise, thus improving the Signal to Noise Ratio (SNR). The standard subcarrier spacing is 15 kHz but, in UL only, it can be reduced down to 3.75 kHz for higher robustness.

To effectively exploit the time-variation of the radio channel, up to 2048 and 128 *repetitions* are allowed in DL and UL, respectively, to increase the success probability of signal reception. Each replica can be decoded separately, or multiple replicas can be combined to further increase the reception probability.

NB-IoT allows flexibility in the cell configuration by defining three *coverage classes*: *Normal* (N), *Robust* (R) and *Extreme* (E).

In order to choose in which coverage class to belong to, an UE performs a measurement of the received power from the evolved Node Basestation (eNB). The outcome is compared with two thresholds, Th_1 and Th_2, defining three possible intervals ($Th_2 < Th_1$). Th_1 separates the interval of received powers associated with class Normal from the one associated with class Robust, whereas Th_2 the interval associated with class Robust from the one associated with class Extreme. Such thresholds depend on the cell deployment, the propagation environment (i.e., outdoor, indoor, deep-indoor, underground) and the spatial distribution of devices. The number of repetitions and network parameters can be tuned separately for each class, as explained in the remainder of the paper.

4.2.2 Deployment and Numerology

The channel bandwidth of NB-IoT is 180 kHz, i.e., one LTE Physical Resource Block (PRB). Three deployment options are available: *standalone*, re-using unused

200 kHz GSM bands; *guard-band*, exploiting the guard band of two adjacent LTE carriers; *in-band*, where one LTE PRB is reserved for NB-IoT within a LTE carrier bigger than 1.4 MHz.

For the sake of coexistence, NB-IoT numerology[1] is inherited from LTE. In both DL and UL, the channel is divided into 12 subcarriers of 15 kHz each. The time domain is divided into *time slots*, each lasting 0.5 ms and consisting of 7 Orthogonal Frequency-Division Multiplexing (OFDM)/Single Carrier Frequency Division Multiple Access (SC-FDMA) symbols. The smallest time-frequency resource, namely Resource Element (RE), is composed of one subcarrier and one symbol. Time slots are grouped as follows: two time slots form one *subframe* (1 ms), 10 subframes form one *frame* (10 ms). Frames are identified by a system frame number, reset every 1024 frames. This structure is then repeated 1024 times, forming the *hyper frame* lasting ∼3 hours.

To further improve the coverage, a second numerology with 48 subcarriers of 3.75 kHz each is introduced. This numerology is used for the preamble transmission of the Random Access Procedure (RAP) (Section 4.2.6) and optionally for UL transmissions. In this numerology, the time slot lasts 2 ms and, for the sake of compatibility, one frame is composed of 5 time slots.

4.2.3 Overview of Signals and Channels

The Narrowband Primary Synchronization Signal (NPSS) is used for initial time-frequency synchronization of the device in the DL. The NPSS is always transmitted on subframe #5 of every frame. The Narrowband Secondary Synchronization Signal (NSSS) is used to accomplish full DL synchronization and obtain information regarding the cell identity, such as the physical Narrowband Cell ID (NCellID). The NSSS is transmitted in subframe #9 of every even frame.

NB-IoT uses the Narrowband Reference Signal (NRS) as a reference point for the DL power as well as channel estimation. It can be transmitted in either one or two

[1] numerical relationships between all the time-frequency variables

antennas and eight REs per subframe are allocated to each antenna. In the special case of the in-band deployment the Cell-specific Reference Signal (CRS), i.e., the LTE reference signal, is also present and the locations of NRS and CRS are derived from the NCellID.

NB-IoT defines the following physical channels, depicted in Fig. 4.2:

- Narrowband Physical Broadcast Channel (NPBCH), used to broadcast information about cell and network configuration;
- Narrowband Physical Downlink Control Channel (NPDCCH), transfers all the control signals from the eNB to the UE;
- Narrowband Physical Downlink Shared Channel (NPDSCH), used for data transmission from the eNB to the UE;
- Narrowband Physical Random Access Channel (NPRACH), used to initiate the RAP;
- Narrowband Physical Uplink Shared Channel (NPUSCH), used for data transmission from the UE to the eNB.

In all subframes, the first two or three REs are reserved for the LTE Physical Downlink Control Channel (PDCCH) to allow interoperability for in-band deployments. One single Hybrid Automatic Repeat reQuest (HARQ) process is used for NPUSCH and NPDSCH.

4.2.4 Power Saving Techniques

In addition to reducing the maximum transmission power from 23 dBm (Class 3) to 14 dBm (Class 6), NB-IoT introduces two power saving techniques: the extended DRX (eDRX) (initially for LTE Cat. M1 in Release 12) and the Power Saving Mode (PSM).

In idle state, the UE periodically monitors the paging channel to check for incoming data. This periodicity, i.e., the Discontinuous Reception (DRX) cycle, has been

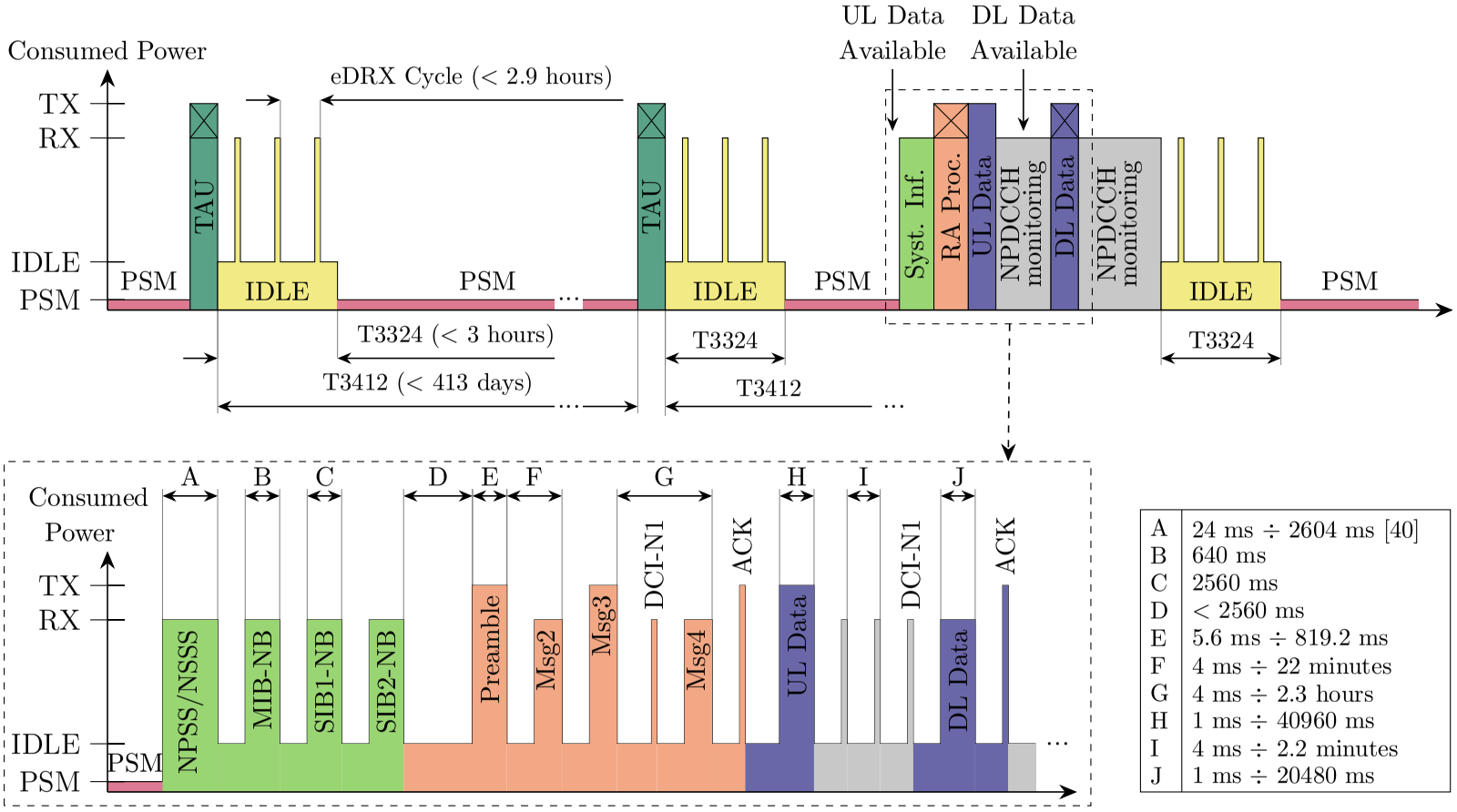

Fig. 4.1: Life-cycle and related power levels of a NB-IoT UE: TAU, idle state with eDRX, PSM, and data transmission with a detailed insight of the RAP. We assume that the UE receives an application acknowledgment before switching to PSM after a UL data transmission.

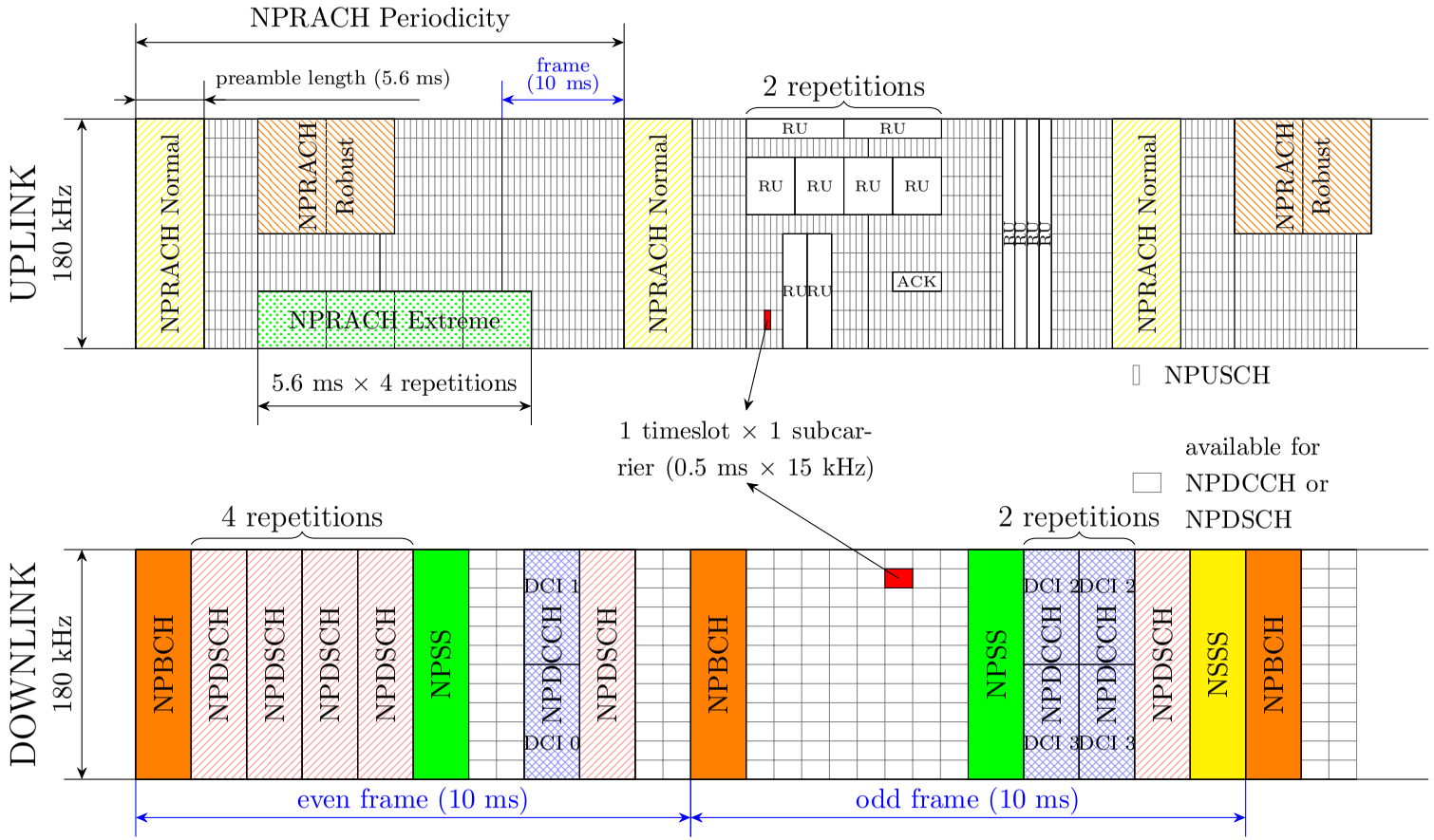

Fig. 4.2: Representation of NB-IoT UL and DL physical channels, assuming 15 kHz subcarriers in UL, Format 0 preamble and two DCI in every NPDCCH subframe.

extended from 2.56 sec (maximum value in LTE) up to a maximum eDRX of ∼175 minutes in NB-IoT.

A UE might also be allowed by the network to switch in PSM. While in PSM, the UE is registered with the network but not reachable (i.e., the paging channel is not monitored with further energy savings with respect to the idle state). At the expiration of the PSM cycle, the UE performs a Tracking Area Update (TAU).

Two timers are defined for the idle and PSM phases: T3324 is the duration of the idle phase (up to ∼3 hours) and T3412 represents the TAU periodicity and thus determines the duration of the PSM cycle (up to ∼413 days) [38], [5]. Fig. 4.1 shows an example of a complete PSM cycle without any activity followed by an activation to transmit data. The aforementioned timers are also listed in Table 4.1.

4.2.5 Downlink Direction

Channels and Related Configurations

In DL only 15 kHz subcarrier spacing is used and QPSK is used in all channels.

The NPBCH always occupies subframe #0 and carries the Narrowband Master Information Block (MIB-NB) which delivers information such as the system bandwidth, the system frame number, the number of antennas ports, and the scheduling for the Narrowband System Information Block 1 (SIB1-NB). The MIB-NB is split into 8 blocks and each block is consecutively repeated 8 times. The overall transmission period of the MIB-NB is 640 ms. Apart from the subframes allocated to NPBCH and NPSS/NSSS (Sec. 4.2.3), the rest of the DL subframes are dynamically allocated to either NPDCCH or NPDSCH.

The NPDCCH carries the Downlink Control Information (DCI) for both data reception and transmission with related number of repetitions to be used. NB-IoT has three DCI formats: N0, used for UL grant; N1, used for DL scheduling; N2, used for paging. NB-IoT also defines NPDCCH format 0 and 1. Each NPDCCH subframe can be split in one or two Narrowband Control Channel Element (NCCE),

each occupying 6 consecutive subcarriers. NPDCCH format 0 uses one NCCE while NPDCCH format 1 can have both NCCE in the same subframe for more robust transmissions. The possible locations of the NPDCCH are called search spaces and three different types are defined: type-1, used for paging; type-2, used for the RAP; type-3, the user-specific search space where UEs can find DL data or control information such as UL grants. To find out if the NPDCCH carries any data for it, a UE uses the appropriate Radio Network Temporary Identifier (RNTI) (specifically P-RNTI for type-1, RA-RNTI for type-2 and C-RNTI for type-3) and looks for it in the NPDCCH's Cyclic Redundancy Check (CRC). For user-specific search space, the periodicity of the NPDCCH occasions vary from 4 ms to 2.2 minutes [35].

The NPDSCH is scheduled in the NPDCCH and is used for dedicated data transmission towards the UE and transmission of Narrowband System Information Blocks (SIB-NBs), containing other system-related information. Examples of SIB-NBs is the SIB1-NB, which provides information such as the Tracking Area Code (TAC), the Public Land Mobile Network (PLMN) identity and the scheduling information for the rest of the SIB-NBs. Its periodicity is 2560 ms and is transmitted in subframe #4 of 16 consecutive even-numbered frames. The transmission can be configured with different Modulation and Coding Schemes (MCSs) (indicated in the MIB-NB) in order to be mapped into 1, 2 or 4 subframes, with 16, 8 or 4 repetitions respectively.

Another example of SIB-NBs is the Narrowband System Information Block 2 (SIB2-NB), which contains the configuration of the paging channel and parameters for the RAP. The periodicity of the SIB2-NB is not specified. The NPDSCH supports a maximum Transport Block Size (TBS) of 680 bits. Depending on the TBS, data transmission can span several subframes.

System Information Acquisition, Paging and Data Reception

The first DL procedure performed by the UE is the synchronization and acquisition of *system information*. By decoding the MIB-NB and at least SIB1-NB and SIB2-NB, the UE retrieves cell and access configurations. As analyzed in [40], the time

required for the synchronization varies from 24 ms to 2604 ms for the best and worst propagation conditions, respectively.

To reach a UE in idle state, the network sends a *paging* message to it via the NPDSCH with DCI format N2. The paging message also indicates whether the paging is done to initiate a request for an Radio Resource Control (RRC) connection (i.e., incoming data) or a change in the system information.

After paging (or if the UE is already connected), the *data reception* can start. The DCI format N1 indicates the resource allocation, the number of subframes that the DL transmission spans, the number of repetitions and the ACK/Not Acknowledgement (NACK) resources to be used. If repetitions are indicated, then identical copies of the data are transmitted by the eNB in consecutive DL subframes excluding subframes used for system information messages using one subframe inter-leaving. If no repetitions are used, the transmission is mapped in continuous DL subframes. If the SIB1-NB is also being transmitted in the frame, the data transmission resumes in the subframe after the one used for the SIB1-NB.

The UE uses the NPUSCH Format 2 (please, refer to section 4.2.6) specified in the DCI to transmit the ACK. Only a single HARQ process is used, and the maximum number of retransmissions is broadcasted by the eNB using the DL_REPETITION_NUMBER-1 of the SIB1-NB. Fig. 4.1 depicts the aforementioned procedures.

The support of SC-PTM was introduced for NB-IoT Release 14 to support multicast transmission.

The SC-PTM is a mix of the unicast transmissions and the Evolved Multimedia Broadcast Multicast Service (eMBMS) framework. Similarly to the eMBMS, the available services for SC-PTM are broadcasted and devices need to subscribe to them in order to receive the content. Upon subscription the device receives a group RNTI (G-RNTI) for the subscribed service. Control information (session start, session stop, resource allocation, etc.) regarding ongoing and upcoming services are carried in the NPDSCH, and are transmitted with a periodicity from 320 ms

to 163.84 seconds [36]. The related location within the NPDSCH is given by the G-RNTI. For data reception, a generic Single Cell Multicast Radio Bearer (SC-MRB) is established and UEs receive the multicast content in a similar way as for UE-specific unicast transmission using their G-RNTI.

4.2.6 Uplink Direction

Channels and Related Configurations

Only two channels are defined in the UL, the NPRACH and the NPUSCH. The NPRACH is used to trigger the RAP. It is composed of a contiguous set of either 12, 24, 36 or 48 subcarriers with 3.75 kHz spacing, which are repeated with a periodicity from 40 ms to 2560 ms. The RAP starts with the transmission of a *preamble*, with a duration of either 5.6 ms or 6.4 ms (Format 0 and 1, respectively, denoted as τ_p) depending on the size of the cell, and can be repeated up to 128 times to improve coverage. A preamble is composed of four symbol groups, each transmitted on a different subcarrier. The first subcarrier is chosen randomly, while the following ones are determined according to a deterministic sequence that depends on the initial subcarrier. Two UEs selecting the same initial subcarrier, will thus collide for the entire sequence. Hence, in each NPRACH occurrence there is a number of orthogonal preambles equal to the number of subcarriers allocated to the NPRACH [8].

The number of repetitions (R_c), the periodicity (T_c) and the number of subcarriers (S_c) allocated to a given NPRACH are defind for each coverage class ($c \in C \equiv \{N, R, E\}$). By choosing an appropriate configuration of the aforementioned parameters and different time offsets it is possible to fit the three NPRACHs without overlaps, each with its own capacity in terms of available preambles (or accesses) per second. We denote this capacity with $Z_c = S_c/T_c$. Fig. 4.2 presents an example of three NPRACHs configured as follows: 48 subcarriers, one repetition, 40 ms periodicity for the Normal class; 24 subcarriers, 2 repetitions, 80 ms periodicity for the Robust class; 12 subcarriers, 4 repetitions, 160 ms periodicity for the Extreme

class.

The NPUSCH occupies all the UL resources left available after the allocation of the NPRACH. NPUSCH format 1 is used for UL data while NPUSCH format 2 carries Uplink Control Information (UCI), which is a DL HARQ ACK in Release 13. Only BPSK or QPSK can be used and the code rate is 1/3 for data transmission and 1/16 for DL HARQ ACK. For UL data, a UE can either use a single or multiple subcarriers (single- and multi-tone capability respectively). To perform a UL transmission, the eNB allocates a certain amount of resources to the UE. The minimum amount of resources is called Resource Unit (RU), where the possible RU configurations [8] depend on the UE capabilities and the configured numerology, and affect the latency as listed in Table 4.1. In the worst case of 3.75 kHz spacing and single-tone capabilities, the only RU that can be used is 32 ms long with either BPSK or QPSK. In the best case of multi-tone capabilities and 15 kHz spacing, a RU is composed of 12 subcarriers and 2 time slots with QPSK. In Fig. 4.2 all the possible RU sizes both for Format 1 and Format 2 are shown assuming a 15 kHz subcarrier spacing. Given the used TBS (up to 1000 bits), the number of required RUs (N_{RU}) depends on the MCS used to meet a certain success probability target, where the relationship between MCS, TBS and number of required RUs can be found in [35]. From a latency point of view, the overall duration of a transmission on the NPUSCH is thus affected by the number of repetitions, the amount of required RU and their configuration (Table 4.1).

Procedures for RA and Data Transmission

The initial procedure in the UL is the RAP, which can be triggered either as a response to a paging message or as UE-initiated procedure for UL data transmission. In order to trigger the RAP, the UE needs to be aware of the system configuration. If the UE is in idle state, it already has that information, while if it is in the PSM mode it first has to retrieve the MIB-NB, SIB1-NB, and SIB2-NB (Sec. 4.2.5).

The RAP comprises of four messages and starts with the transmission of a preamble (Msg1) on the first available NPRACH opportunity (Section 4.2.6). If multiple UEs

choose the same initial subcarrier the preamble sequence will collide but the eNB is not yet aware of it. After the preamble transmission the UE starts a Random Access Response (RAR) window, which lasts from 2 to 10 times the NPDCCH period (Sec. 4.2.5). During this time, the UE expects to receive the RAR message (i.e., Msg2) through the NPDSCH which indicates the preambles identified by the eNB. The RA-RNTI univocally identifies the preambles and lets the UEs identify if the RAR is addressed to it. For each preamble listed in the RAR, the eNB provides a UL grant for the transmission of Msg3 of the RAP. The maximum number of preambles that can be addressed for each RAR is a network-specific value and it is used to moderate the load. The UEs that did not receive the Msg2 within their RAR window will perform a new RAP attempt. In this phase, colliding UEs will receive the same RAR without being aware that a collision happened. After Msg2 reception, the UE transmits the Msg3 on the NPUSCH according to the UL grant received in Msg2. The Msg3 carries information such as the UE identity and the Buffer Size Report (BSR). The UE now starts a Contention Resolution Timer (from 1 to 64 times the NPDCCH period long, Section 4.2.5), during which it expects to receive the Msg4 on the NPDSCH. The Msg4 carries the UL grant to be used for data transmission and it is also used to resolve the collisions. The Msg3 and Msg4 are transmitted using HARQ through the NPUSCH and NPDSCH respectively.

If the RAP fails in any of the aforementioned phases, the UE performs a new attempt after a backoff time of up to ∼9 minutes. If the UE reaches the maximum number of attempts (A_c, configured by the network and up to 10), it will keep trying in another coverage class. A maximum total number of attempts up to 200 can be configured and after reaching it the UE declares a RAP failure. The aforementioned parameters (i.e., RAR window, timers, backoff value, maximum number of attempts) could also be specified for each coverage class separately. Latency components of the RAP are summarised in Table 4.1.

Once resources have been granted with the reception of Msg4, the UE starts transmitting its payload on the NPUSCH using HARQ. ACK/NACK for the HARQ are carried within the UL, where the New Data Indicator (NDI) bit is exploited for this

purpose. The NDI bit is used to distinguish the request for a new transmission from a request for retransmission of the previous packet. In case of failure, the eNB will send another UL grant where the NDI bit will be exploited as a NACK and the UL grant will inform the UE about the resources assigned for the retransmission. Up to 28 retransmissions are considered for the NPUSCH. The eNB can also instruct a UE to perform each retransmission using different versions of the redundancy bits using the "redundancy version" in the UL, in order to improve the success probability [35, 34]. Fig. 4.1 shows an example of a complete procedure followed by a non-synchronised UE in order to transmit a data packet (all steps of the RAP and data transmission/reception are assumed to be successful).

Source of Latency	**Influenced by**	**Description**
eDRX [5]	• DRX cycle periodicity (< 175 minutes)	• The DRX cycle periodicity affects the time for DL reachability
Power Saving Mode [5]	• Idle timer (T3324) < 3 hours • PSM timer (T3412) < 413 days	• T3324 and DRX cycle periodicity define the number of occasions for DL reachability. • T3324 and T3412 define how long the UE will not be reachable.
Initial Synchronization [40]	• Channel Quality • Deployment {inband; standalone}	• Best: 24ms (good channel) • Worst: 2604ms (bad channel, inband)
System Information	• MIB-NB periodicity (640ms) • SIB1-NB periodicity (2560ms) • SIB2-NB periodicity (chosen by the operator) • Channel Quality	• MIB-NB and SIB-NBs need to be decoded in sequence, and therefore the latency is at least equal to the sum of the the related periodicities

NPUSCH Transmission	• Payload Size • Subcarrier Spacing (3.75kHz, 15kHz) • Multi-tone capability • RU chosen by the scheduler • Number of repetitions (1, 2, 4, . . ., 128)	• Numerology and UE capabilities determine the duration of each RU [8] • Best: 1ms (15kHz, multi-tone, shortest RU, 1 repetition, 1 RU) • Worst: 40960ms (3.75kHz, 128 repetitions, 10 RUs)
NPRACH occurrence	• NPRACH Periodicity (40, 80, 160, 240, 320, 640, 1280, 2560) ms • Activation Instant	• Average: half of NPRACH periodicity • Upper Bound: NPRACH periodicity
Preamble Transmission	• Preamble Format (Format 0 or 1) • Number of Repetitions (1, 2, 4, . . ., 128)	• The format depends on the cell size and affect the preamble length (Format 0: 5.6ms; Format 1: 6.4ms) • Best: 5.6ms (Format 0, 1 repetition) • Worst: 819.2ms (Format 1, 128 repetitions)
RA Backoff	• Backoff configuration 256×(0, 1, 2, 4, . . ., 2048) ms	• Uniformly distributed between 0 and the configured value • Worst: 524288ms (∼9 minutes)
NPDCCH Occasion periodicity	• Number of repetitions • Start offset G (1.5, 2, 4, . . . , 64)	• Computed as $max\{R_{max} \cdot G; 4\}$, where R_{max} is the maximum number of repetitions used in the cell and G a time offset [35] • Best: 4ms • Worst: 2.3 minutes

RAR Reception	• Packet Scheduling • NPDCCH Occasion periodicity • RAR Window Size (2, 3, 4, 5, 6, 7, 8, 10)× NPDCCH Occasion periodicity [36]	• Best: 4ms (processing time at eNB and margin to switch from transmission to reception at UE side) • Worst: 22 minutes
Contention Resolution Window	• Packet Scheduling • NPDCCH Occasion periodicity • Contention Resolution Window Size (1, 2, 3, 4, 8, 16, 32, 64) × NPDCCH Occasion periodicity [36]	• Best: 4ms (processing time at eNB side and margin to switch from transmission to reception at UE side) • Worst: 2.3 hours
NPDSCH/NPDCCH Transmission	• Payload Size • Number of Repetitions (1, 2, 4, . . . , 2048)	• Best: 1ms (1 repetition, 1 subframe) • Worst: 20480ms (2048 repetitions, 10 subframes)
HARQ Retransmission	• Transmission Time Interval (TTI) (chosen by the operator)	• Only a retransmission per TTI can be triggered by the HARQ process

Table 4.1: Summary of the main sources of latency.

4.3 Mathematical Model

4.3.1 Scenario and Coverage

We consider the eNBs to be placed in an hexagonal grid with a variable Inter-Site Distance (ISD) each of them forming a three-sectorial site. As described in [2], in a dense urban scenario like the city of London, ISD can be set as 500m.

Nevertheless, the possibility of deploying NB-IoT only in a subset of the eNBs is often considered; thus, ISD may be larger. We approximate the cell as a circle with radius R_{cell}= $\frac{2}{3}$ISD. Fig. 4.3 depicts the aforementioned scenario.

The geometry of a cell, a circle of radius R_{cell} with the eNB in the center, and the actual shape of the cell, an hexagon with the eNB in one vertex and R_{cell} as the maximum distance, are indeed quite different. Nevertheless, the impact of this approximation is limited to the statistics of the user distances for what concerns the mathematical model. The difference between the two cumulative density functions is limited; in particular, the devices in the real cell, on average, tend to be closer to the eNB with respect to the circular approximation, therefore this evaluation can be considered as a worst case.

Depending on the use case considered, the devices, uniformly spread in the cell, are partitioned among outdoor (O), indoor (I) or deep-indoor (DI) deployment conditions with different proportions. We denote as p_d the probability for a device to be deployed in condition d, where $d \in D \equiv \{O, I, DI\}$.

We express the received power at distance r as described in (2.2) with the only difference that the additional penetration loss L_{add} is different for each deployment condition d; thus it is expressed as $L_{add,d}$. The values for this, and any other parameter defined afterwards, are based on the 3GPP London path loss model described in Table 2.1; they are also reported in Table 4.2.

The UE and the eNB have different transmit powers, different antenna gains and cable losses; thus, the parameter P_{r0} can be either $P_{\mathrm{r0}}^{\mathrm{UL}}$ when the uplink is considered, or $P_{\mathrm{r0}}^{\mathrm{DL}}$ when the downlink is considered.

Firstly, I compute the probability for a device deployed in condition d to choose coverage class c, as a function of distance, which I denote as $p_{c,d}^{CLASS}(r)$. The received power from the eNB is compared to the aforementioned decision thresholds Th_c. The probability of choosing a given coverage class is equal to the probability of the received power to be higher than the corresponding threshold, minus the probability of choosing one of the coverage classes characterised by higher threshold. In other

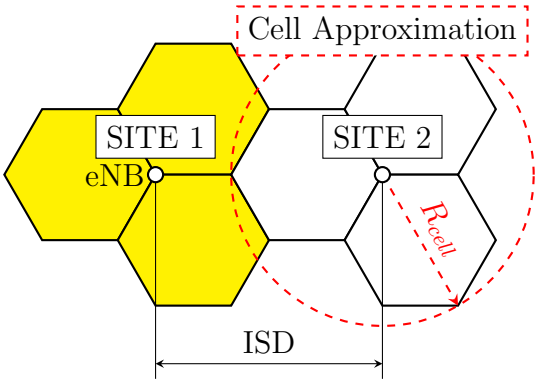

Fig. 4.3: Reference deployment scenario and relation between the ISD and the cell radius (R_{cell}).

words, the probability is computed as in (4.1), where the values of the index c can be equal to 1, 2 and 3 representing respectively coverage classes Normal, Robust and Extreme, while $Th_3 = -\infty$.

$$p_{c,d}^{CLASS}(r) = \mathbb{P}\left\{P_{r,d}^{DL}(r) > Th_c\right\} - \sum_{i=1}^{c-1} p_{i,d}^{CLASS}(r) \tag{4.1}$$

By inserting the expression for the received power the final expression for this probability can be derived(4.2).

$$p_{c,d}^{\text{CLASS}}(r) = \frac{1}{2}\text{erfc}\left(\frac{Th_c - P_{r0}^{\text{DL}} + 10\beta\log(r) + L_{add,d}}{\sigma_S\sqrt{2}}\right) - \sum_{i=1}^{c-1} p_{i,d}^{\text{CLASS}}(r) \tag{4.2}$$

Then, it is possible to compute the probabilities for any device in a random position within the cell to belong to a given coverage class, by averaging for each deployment condition and integrating across the circular area the aforementioned equation. (4.3) shows the resulting expression assuming a uniform distribution of the UEs.

$$p_c^{CLASS} = \frac{2}{{R_{cell}}^2}\sum_{d\in D} p_d \int_0^{R_{cell}} p_{c,d}^{CLASS}(r) r dr \tag{4.3}$$

The coverage probability is one of the metrics used to evaluate the performance of

the system. It is computed as the fraction of devices configured with a number of repetitions sufficiently high to be decoded correctly by the eNB. In [41] the authors show the average number of repetitions required to decode the NPUSCH transport block as a function of the SNR, in presence or absence of doppler spread (f_d), and for different MCSs. Since in that paper only the average number of repetitions has been estimated, it is not possible to define a minimum requirement. Thus, I assume that the average corresponds to the minimum requirement ($R_{\min}$) with a consequent overestimation of the coverage probability. Considering an effective noise power of $-129\ dBm$ [2], and assuming $f_d = 0\ Hz$ and $MCS_{index} = 0$, the selected curve in [41] can be approximated as $R_{\min}(r) = 2^{-A \cdot P_r^{UL}(r) - B}$ where A= 0.2902 and B= 37.25.

The coverage probability at a given distance from the base station, and for a given coverage class and deployment condition ($p_{c,d}^{\mathrm{COV}}(r)$), can be computed as the probability of having a received power such that the number of repetitions configured is higher than $R_{\min}$; this leads to (4.4).

$$\begin{aligned} p_{c,d}^{\mathrm{COV}}(r) &= \mathbb{P}\left\{R_{\min}(r) < R_c\right\} = \\ &= \frac{1}{2}\mathrm{erfc}\left(\frac{10A\beta\log_{10} r - \log_2 R_c - A\left(P_{\mathrm{r0}}^{\mathrm{UL}} - L_{add,d}\right) - B}{A\sigma_S\sqrt{2}}\right) \end{aligned} \tag{4.4}$$

Finally, in order to estimate the amount of traffic actually processed by the eNB in a certain coverage class, we need to compute $p_{c,e}^{\mathrm{CONN}}$ that represents the probability, for a device at a certain distance and in deployment condition d, to be connected to the eNB and configured in coverage class c at the same time (4.5).

$$p_{c,d}^{\mathrm{CONN}} = \frac{2}{{R_{\mathrm{cell}}}^2}\int_0^{R_{\mathrm{cell}}} p_{c,d}^{\mathrm{CLASS}}(r) p_{c,d}^{\mathrm{COV}}(r) r dr \tag{4.5}$$

The actual percentage of devices connected to each coverage class can be computed as in (4.6). Notice that $\sum_{c\in C} p_c^{\mathrm{CONN}} < 1$; in fact, some devices are not connected at all to the eNB.

$$p_c^{\mathrm{CONN}} = \sum_{d \in D} p_d p_{c,d}^{\mathrm{CONN}} \tag{4.6}$$

4.3.2 Traffic Estimation

In this section I assume all the UEs to implement to the same application and performing the same access pattern, characterised by an overall offered traffic in UL, of O packets per second, each of them with a payload of P_L bytes. For this part of the model I temporarily ignore the devices which are not connected; I define in (4.7) a second set of probabilities, $p_c^{\mathrm{CONN}'}$, which are a normalised version of p_c^{CONN}. In this way I consider only the connected devices and their relative proportions. With this definition, the equivalences reported in (4.8) are valid for later use.

$$p_c^{\mathrm{CONN}'} = \frac{p_c^{\mathrm{CONN}}}{\sum_{c \in C} p_c^{\mathrm{CONN}}} \tag{4.7}$$

$$O'_c = p_c^{\mathrm{CONN}'} O' = p_c^{\mathrm{CONN}} O \tag{4.8}$$

We assume that the RAPs performed by devices belonging to the same coverage class are handled independently from the other classes. We denote as $N_{p,c}$ the average number of preambles sent in each occurrence of the NPRACH for coverage class c. Assuming that the distribution of the preamble transmissions is a Poisson process, and that the probability of choosing a given initial subcarrier is $1/S_c$, I can compute the probability of having one or more UEs starting the preamble with a certain subcarrier as in (4.9).

$$p_{\mathrm{SC,c}} = 1 - e^{-\frac{N_{p,c}}{S_c}} \tag{4.9}$$

We assume that Msg2, Msg3 and Msg4 are always transmitted successfully once the preamble is received, and that HARQ is not used. The number of successful accesses, or the number of Msg2 sent, is then equal to the number of subcarriers used

by at least one UE at the beginning of the preamble (each set of colliding preambles will be seen as a single one from the point of view of the eNB and only one UE will complete the RAP successfully). In a mathematical form, $N_{s,c} = p_{\mathrm{SC},c} S_c$. Since the NPRACHs have a different periodicity for each coverage class, we should express the same concept employing a common time unit (one second). $O'_{p,c} = \frac{N_{p,c}}{T_c}$ and $O'_{s,c} = \frac{N_{s,c}}{T_c}$ denote the number of preambles sent and the number of successful accesses per second, respectively. Their relation is shown in (4.10).

$$O'_{s,c} = Z_c \left(1 - e^{-\frac{O'_{p,c}}{Z_c}}\right) \tag{4.10}$$

The number of preambles actually sent is equal to the number of devices that start the RAP (O'_c) plus the number of devices performing another attempt after failing the previous ones ($O'_{r,c}$). The latter can be computed as $O'_{r,c} = O'_{p,c} - O'_{s,c} - O'_{f,c}$ where $O'_{f,c}$ denotes the number of devices which failed the RAP after A_c attempts and can be computed as shown in (4.11).

$$O'_{f,c} = O' p_c^{\mathrm{CONN}'} \left[1 - \frac{Z_c}{O'_{p,c}} \left(1 - e^{-\frac{O'_{p,c}}{Z_c}}\right)\right]^{A_c} \tag{4.11}$$

Finally, this information can be merged in (4.12) that can be solved numerically for $O'_{s,c}$. Notice that $O'_{s,c} \in [0, Z_c]$, therefore the solution to this equation can be computed using a simple iterative bisection algorithm. The relation between O' and $O'_{s,c}$ can be represented as a function denoted as $O'_{s,c} = O_{s,c}(O')$.

$$O'_{s,c} + O'_c \left[1 + \frac{O'_{s,c}}{Z_c \log\left(1 - \frac{O'_{s,c}}{Z_c}\right)}\right]^{A_c} = O'_c \tag{4.12}$$

Although the NPRACH is able to accept successfully up to Z_c connections, the actual maximum number of transmissions possible may be smaller if the radio resources on the NPUSCH are depleted earlier. To take into account the actual size of the NPUSCH, I denote with *uplink occupation coefficient* (ρ_{UL}) the ratio between the amount of radio resources used for the transmission of any packet and the

resources available in the NPUSCH. In (4.13) it is shown how to compute this coefficient assuming that for each successful access a data packet and a Msg3, occupying three RUs, are transmitted through the NPUSCH.

$$\rho_{\mathrm{UL}} = \underbrace{\frac{2S_{\mathrm{RU}}\tau_{\mathrm{RU}}\left(3+N_{\mathrm{RU}}(P_L)\right)}{24000-\frac{1}{2}\sum_{c\in C} Z_c\left\lceil \tau_p R_c\right\rceil}}_{1/W} \sum_{c\in C} R_c O_{s,c}(O') \tag{4.13}$$

S_{RU} and τ_{RU} are respectively the number of subcarriers and the duration in milliseconds of the RU used in the NPUSCH, $N_{RU}(P_L)$ is the number of RUs that the transmission of P_L bytes requires as mentioned in Section 4.2. Also, in (4.13), the term $N_{RU}(P_L)$ is summed with 3, this represent the number of RUs used for Msg3 transmission.

The network is considered saturated if the coefficient becomes bigger than one; this is, in a mathematical form, equivalent to (4.14).

$$\sum_{c\in C} R_c O_{s,c}(O') > W \tag{4.14}$$

Since the maximum value of $O_{s,c}(O')$ is Z_c, we can have two possible cases. When $\sum_{c\in C} R_c Z_c < W$, it means that the NPUSCH will never be saturated because the NPRACH is small enough to have a considerable amount of collisions which does not allow to occupy all the NPUSCH resources with the few successful transmissions. Otherwise, it exists an amount of offered traffic $\hat{O}'$ which saturates the NPUSCH. In the first case the only way to have the maximum throughput is with an infinite offered traffic, which would lead to a success probability equal to 0; due to the criteria used to evaluate the performance defined in Section 4.5, we decided to ignore this scenario. In the second case the equation $\sum_{c\in C} R_c O_{s,c}(\hat{O}') = W$ must be solved numerically for $\hat{O}'$, then the maximum throughput can be computed as T_{max}= $8P_L \sum_{c\in C} O_{s,c}(\hat{O}')$ *bps*.

The access success probability, when the offered traffic is such that the maximum throughput is reached, can be computed, for each coverage class, as p_c^{MAC}=

$O_{s,c}(\hat{O}')/\hat{O}'_c$.

Finally, in (4.15) I apply the equivalences (4.8) and I compute the overall success probability as the ratio between the sum of all the successful transmissions among the three coverage classes and the offered traffic.

$$\begin{aligned} P_s &= \frac{\sum_{c\in C} O'_{s,c}(\hat{O}')}{\hat{O}} = \frac{\sum_{c\in C} p_c^{\mathrm{MAC}} \hat{O}'_c}{\hat{O}} \\ &= \frac{\sum_{c\in C} p_c^{\mathrm{MAC}} p_c^{\mathrm{CONN}} \hat{O}}{\hat{O}} = \sum_{c\in C} p_c^{\mathrm{MAC}} p_c^{\mathrm{CONN}} \end{aligned} \tag{4.15}$$

4.3.3 Fairness Estimation

In order to fully evaluate the performance of a configuration I define also a metric for the fairness of the quality of service provided to the users. In fact, we want to understand if the network is able to provide a good service also to the devices that are in poor coverage conditions or to evaluate how their performance is different from a device in a good position. The metric used for this scope is the Jain's Index, whose definition is expressed in (2.4).

The fairness is based on the throughput of each individual device in the network (t_i).

In order to define an expression for the Jain's Index based on the metrics defined in the previous section, I consider a circular cell of radius R_{cell} where devices are distributed uniformly with density ρ. d_i, c_i and r_i represent the deployment condition, the coverage class and the distance from the cell of the i-th device respectively. The average number of devices in the cell can be computed as $n = {R_{\mathrm{cell}}}^2 \pi \rho$, while the average number of devices belonging to coverage class c can be computed as $n'_c = n p_c^{\mathrm{CONN}'} = {R_{\mathrm{cell}}}^2 \pi \rho p_c^{\mathrm{CONN}'}$. Assuming to have the network in saturation condition when all the devices transmit a total of $\hat{O}$ packets per second, I can express the throughput experienced by each device as $t_i = \frac{8 P_L \hat{O}}{n} p^{COV}_{c_i,d_i}(r_i) p_c^{\mathrm{MAC}}$.

We can replace the expression for the individual throughput in the definition of the Jain's Index as done in (4.19).

We can split the terms within the summations into multiple sets characterised by the same coverage class index, as done in (4.20). Then we can multiply and divide for n'_c both the numerator and denominator and continue the processing of the expression as done in (4.21).

The two quantities $\frac{1}{n'_c}\sum_{j|c_j=c} p^{COV}_{c,d_j}(r_j)$ and $\frac{1}{n'_c}\sum_{j|c_j=c}(p^{COV}_{c,d_j}(r_j))^2$ represent the average of, respectively, the coverage probability and its square, among all the devices belonging to class c in the cell. We denote these two quantities as $\overline{p_c^{COV}}$ and $\overline{\overline{p_c^{COV}}}$ respectively. Using the definition provided in Section 4.3.1 I found an analytical expression for them which is reported in (4.16) and (4.17) .

$$\overline{p_c^{\mathrm{COV}}} = \frac{2}{{R_{\mathrm{cell}}}^2}\sum_{d\in D} p_d \int_0^{R_{\mathrm{cell}}} p^{\mathrm{COV}}_{c,d}(r) r dr \tag{4.16}$$

$$\overline{\overline{p_c^{\mathrm{COV}}}} = \frac{2}{{R_{\mathrm{cell}}}^2}\sum_{d\in D} p_d \int_0^{R_{\mathrm{cell}}} \left[p^{\mathrm{COV}}_{c,d}(r)\right]^2 r dr \tag{4.17}$$

$$\mathrm{JI} = \frac{\left(\sum_{i=1}^n t_i\right)^2}{n\cdot\sum_{i=1}^n t_i^2} = \tag{4.18}$$

$$= \frac{\left(\frac{8P_L\hat{O}}{n}\right)^2\left(\sum_{i=1}^n p^{\mathrm{COV}}_{c_i,d_i}(r_i)p^{\mathrm{MAC}}_c\right)^2}{n\left(\frac{8P_L\hat{O}}{n}\right)^2\sum_{i=1}^n (p^{\mathrm{COV}}_{c_i,d_i}(r_i)p^{\mathrm{MAC}}_c)^2} = \tag{4.19}$$

$$= \frac{\left(\sum_{c\in C} p^{\mathrm{MAC}}_c \sum_{j|c_j=c} p^{\mathrm{COV}}_{c,d_j}(r_j)\right)^2}{n\sum_{c\in C}\left(p^{\mathrm{MAC}}_c\right)^2\sum_{j|c_j=c}(p^{\mathrm{COV}}_{c,d_j}(r_j))^2} = \tag{4.20}$$

$$= \frac{\left(\sum_{c\in C} p^{\mathrm{MAC}}_c n'_c\frac{1}{n'_c}\sum_{j|c_j=c} p^{\mathrm{COV}}_{c,d_j}(r_j)\right)^2}{n\sum_{c\in C}\left(p^{\mathrm{MAC}}_c\right)^2 n'_c\frac{1}{n'_c}\sum_{j|c_j=c}(p^{\mathrm{COV}}_{c,d_j}(r_j))^2} = \tag{4.21}$$

$$= \frac{\left(\sum_{c\in C} p^{\mathrm{MAC}}_c n'_c\overline{p_c^{\mathrm{COV}}}\right)^2}{n\sum_{c\in C}\left(p^{\mathrm{MAC}}_c\right)^2 n'_c\overline{\overline{p_c^{\mathrm{COV}}}}} = \tag{4.22}$$

$$= \frac{\left(\sum_{c\in C} p^{\mathrm{MAC}}_c p^{\mathrm{CONN}'}_c\overline{p_c^{\mathrm{COV}}}\right)^2}{\sum_{c\in C}\left(p^{\mathrm{MAC}}_c\right)^2 p^{\mathrm{CONN}'}_c\overline{\overline{p_c^{\mathrm{COV}}}}} \tag{4.23}$$

4.4 Performance

In this Section, I provide an insight on the performance of NB-IoT considering some of the realistic use cases described in Chapter 2, each with different UE density, report periodicity (λ) and Payload Size (P_L). Refer to Table 2.6 for their characteristics. The presented results are produced through the mathematical model described in Section 4.3. Each use case has a different percentage of UEs in outdoor, indoor, and deep indoor conditions, that determines the percentage of UEs in Normal, Extended and Extreme classes. The total overhead (considering User Datagram Protocol (UDP)/Internet Protocol (IP) and 3GPP protocol stack) is 65 B. UEs randomly wake up considering their λ, decode MIB-NB, SIB1-NB and SIB2-NB, perform the RAP to send a UL report, then receive a 30 B DL packet (when still connected) representing an application-level acknowledgment. Other documents describing typical use cases are available (e.g.: [42]) but the differences, for the sake of the results presented in this work, are marginal. For the sake of simplicity I consider one use case at a time and I assume a stationary regime where the offered traffic and the network conditions are constant over time. This set of use cases covers a wide range of traffic amounts, from 5 to 12000 packets per hour per cell. Peaks of traffic cannot be evaluated due to limitations of the model used; nevertheless, under the assumption of the peak duration being longer than the duration of the transient triggered by the new conditions, the resulting performance would be equivalent to having a stable traffic of the same entity of the peak.

The deployment scenario considered is described in Section 4.3.1. The number of repetitions used is computed considering -100 dB and -110 dB as the received signal power thresholds for the coverage classes definition, their worst case Signal to Interference plus Noise Ratio (SINR) and the results reported in [41].

4.4.1 Analysis of Realistic Use Cases

The percentages of Uplink and Downlink channel utilization for each use case and ISD analyzed are reported in Fig. 4.4, which also shows how UL and DL resources

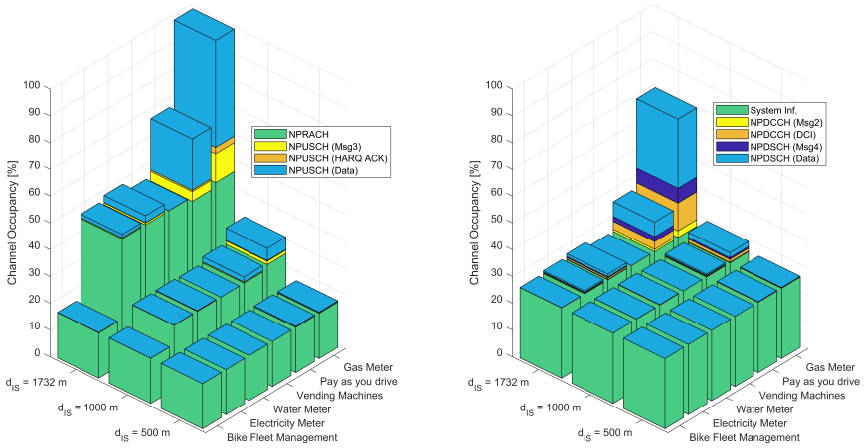

Fig. 4.4: Channel occupancy in UL (left) and DL (right) directions for different realistic use cases and NPRACH configured with 12 subcarriers and 40, 640, 640 ms periodicity for the three coverage classes.

are divided across the different message types. We can observe that the amount of resources used for the NPRACH increases as the ISD increases. This is due to the fact that the number of repetitions used in the three coverage classes increases in the same way in order to satisfy the UEs on the edge of the bigger cell. In some cases, such as the Bike Fleet Management, the devices are deployed mostly outdoor, so they experience a better channel on average. Therefore, the number of repetition can be kept low with a consequent lower occupancy of the radio resources. The amount of resources used for the data transmission through the NPUSCH also increases as the cell becomes larger. This is due to the higher number of repetitions and to the higher number of UEs covered by the bigger cell. Nevertheless, we can observe that in most use cases, a single NB-IoT carrier is sufficient to manage all the traffic, in most cases with a very large margin. However, for Gas Metering with ISD= 1732 m the network is almost saturated in the UL. As a first approximation for each data transmission there is a corresponding Msg3 transmission. Although the payload of this message is much smaller with respect to the application data the amount of resources used for both messages are proportional to the traffic. Finally, the resources consumed by the Format 2 ACKs of the DL HARQ processes for Msg4 and data transmission are generally negligible. Around 25% of DL resources are

used for the transmission of the NPSS, NSSS, MIB-NB, SIB1-NB and SIB2-NB. The remaining resources are mostly used for DL data and a smaller amount is used for Msg2, Msg4 and the DCIs transmitted in the various phases while the UE is active. As expected, the UL is always more loaded w.r.t. DL, given to the different payload size in the two directions.

4.4.2 Firmware Update Use-Case With Unicast and SC-PTM Transmissions

We considered a firmware update of 1 MB being transmitted to 50 devices. To transmit the firmware update, I used only the resources remained free after considering the transmission of DL background traffic related to application acknowledgments as described above. We also assumed that each UE receives the update independently from other devices for unicast transmission, while UEs are receiving the firmware simultaneously for the SC-PTM case. We considered pay-as-you-drive and gas meters applications as two examples of use cases with limited and high resource utilization, respectively.

The results reported in Fig. 4.5 focus on the firmware update delivery time, computed as the time interval from the moment the firmware update is started to be transmitted to the first UE to the moment the last UE receives the update. The analysis shows that the total time required to deliver the update to all of the 50 UEs increases as the ISD increases. When UEs are deployed within a 500 m cell, the firmware delivery time does not present significant differences between the different use cases, compared to the differences observed when the ISD is 1732 m. This is expected as devices that are placed further away from the cell center experience greater propagation loss and require more repetitions based on their coverage class. Similarly to the previous results, the Gas Metering use case is the one that requires the longest delivery time due to the amount of traffic generated, regardless of the ISD. In the case of SC-PTM the introduced gains in terms of delivery time are quite obvious w.r.t. unicast, although it is worth mentioning that for unicast mode the

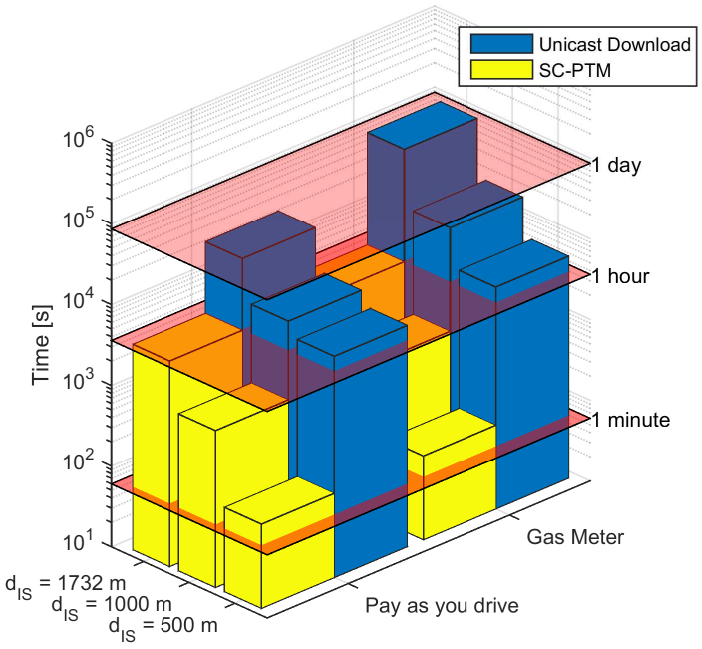

Fig. 4.5: Firmware update delivery time to 50 devices with unicast and SC-PTM modes for pay-as-you-drive and gas meters use cases.

delivery time varies from the order of hours to 1 day (i.e., ∼24 times higher) when increasing the ISD from 500 m to 1732 m, while it varies from the order of minutes to 1 hour (i.e., ∼60 times higher) for the SC-PTM. This indicates that the effective gains of SC-PTM w.r.t. unicast mode are strictly related to the location of UEs. Nevertheless, it is worth underlining that while the delivery time is affected by the number of UEs in the unicast case, the SC-PTM has a performance that does not vary with the number of UEs being served. Thus, the choice of using either unicast or SC-PTM depends on the number of UEs to be served and their coverage class.

4.5 Network Configuration Optimization

The optimal configuration of the network depends on the definition of some performance metrics and on what we consider to be optimal. The model presented in Section 4.3 can be easily adapted to provide many different performance met-

rics. For the sake of simplicity I decided to evaluate each possible configuration of the network based on the maximum throughput possible, the global success rate achieved with that throughput (4.15) and the Jain's Index (4.23).

The configuration parameters of interest are nine: the number of repetitions for the three coverage classes (R_c), the number of preambles per seconds available in each NPRACH for the three coverage classes (Z_c), the two thresholds for the coverage class decision (Th_1, Th_2) and the inter-site distance (ISD).

The amount of possible configurations is huge, therefore I decided to estimate the performance metrics choosing randomly a large set of possible inputs with a Monte Carlo approach. In this paper I consider a scenario characterised by UEs deployed mostly outdoor ($[p_{\mathrm{O}}, p_{\mathrm{I}}, p_{\mathrm{DI}}] = [0.6, 0.3, 0.1]$). The values of the remaining parameters are reported in Table 4.2. The possible values of the model inputs are chosen in the following sets: $R_c \in \{1, 2, 4, 8, 16, 32, 64, 128\}$, $Th_1, Th_2 \in$ [-150, 50] dBm, $Z_c \in \{48/0.04, 24/0.04, 12/0.04, 12/0.08, 12/0.16, 12/0.24, 12/0.32, 12/0.64, 12/1.28, 12/2.56\}$. Although the inter-site distance is 500m, as I mentioned in the previous sections, the operator may want to deploy NB-IoT only in a subset of the eNBs. For this reason I impose to have a specific inter-site distance, 1732m in the first set of results (one NB-IoT site every 12 LTE sites). We generated 10^5 different configurations, then I represented each outcome as a point in a two dimensional plane where each coordinate represents one of the performance metrics estimated.

Fig. 4.6 represents the success probabilities and maximum throughputs obtainable with ISD= $1732m$. It is possible to notice, as expected, that a random configuration, generally, provide a very poor performance. Most of the configurations are concentrated on the left side of the figure, characterised by a maximum throughput lower than 30 kbps. Very few configurations provide a high throughput and success rate at the same time.

An operator may decide to adopt different definitions of "best performance" based on these results according to its needs. For instance, the maximum throughput alone is a too simplistic criteria to use, as often the configurations with the highest throughput lead to a very low success probability. We propose to define the best

Symbol	Description	Value	Unit
	Channel and Deployment		
$P_{\text{r0}}^{\text{UL}}$	Received power at 1 km in UL	-86.9	dBm
$P_{\text{r0}}^{\text{DL}}$	Received power at 1 km in DL	-66.9	dBm
β	Path Loss exponent	3.76	-
σ_S	Shadowing standard deviation	8	dB
$L_{add,d}$	Additional loss $[O, I, DI]$	$[0, 20, 40]$	dB
	NPUSCH		
S_{RU}	RU number of subcarriers	1	-
τ_{RU}	RU duration	8	ms
A	Required repetitions approximation parameter	0.2902	-
B	Required repetitions approximation parameter	37.25	-
	NPRACH		
τ_p	Preamble Repetition Length	5.6	ms
A_c	Maximum number of RAP attempts $[N, R, E]$	$[3, 3, 3]$	-
	Application		
P_L	UL data payload	50	B
$N_{RU}(P_L)$	Number of RUs needed	8	-

Table 4.2: Summary of the model parameters and their values [8, 2].

configuration as the one providing the highest T_{max} and P_s>1−$P_{e,max}$ at the same time, with $P_{e,max}$= 10%.

According to this definition, the maximum throughput achievable in this scenario is 52.4 kbps with a success probability of 96% and a Jain's index of 0.99, performance obtainable with the configuration reported in Table 4.3.

By observing p_c^{CONN}, it is possible to see that Th_1 and Th_2 are chosen in a way that almost all devices belong to coverage class Robust, which implies one repetition. The reason is that with ISD= $1732m$ the coverage is generally quite good even with only one repetition; for instance, in this scenario only few devices in deep-indoor conditions at more than 700m from the eNB are not covered (2.5% of all the devices). In this case the best solution is to avoid allocating resources for two additional coverage classes in order to maximise the capacity of the NPUSCH; in

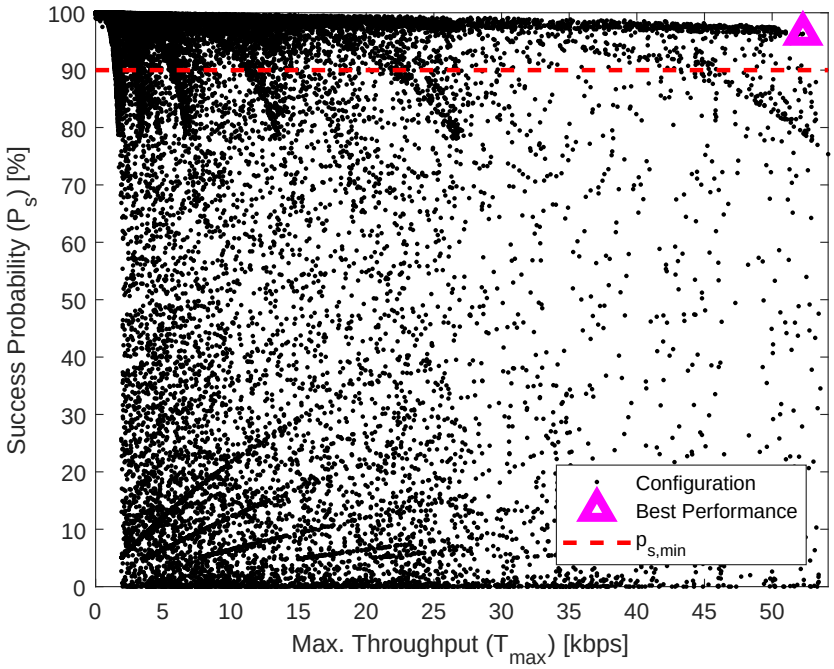

Fig. 4.6: Performance of a NB-IoT network with random generated configurations and $ISD = 1732m$.

fact the two NPRACHs associated with class Normal and Extreme are as small as possible since almost no traffic is carried by them ($Z_N = Z_E = 12/2.56 = 4.68$ *preambles*/*second*). Ideally the operator may decide to completely switch off the additional coverage classes in such scenario to further improve the NPUSCH capacity.

In Fig. 4.7 we can observe the relationship between the Jain's Index and the maximum throughput possible in the scenario mentioned. The best configuration already provides a close-to-best throughput and fairness even if there is room for improvements, provided that the success rate requirement is relaxed.

As already mentioned, in this scenario one repetition is sufficient to cover almost all the devices deployed; therefore, having an inter site distance of 1732m is not particularly challenging from the coverage point of view. In order to stress the system, I considered a second scenario characterised by ISD= $3464m$ (one NB-IoT site every 48 LTE sites).

	Best Performance (ISD= $1732m$)		
	N	***R***	***E***
p_c^{CONN}	3.4%	94%	0.07%
p_c^{MAC}	84%	99%	100%
T_{max}	52.4 kbps		
P_s	96%		
JI	0.99		
	Configuration		
R_c	1	1	2
T_c	2.56 s	0.04 s	2.56 s
S_c	12	12	12
Th_1	-13 dBm		
Th_2	-126 dBm		

Table 4.3: Best performance and network configuration for $ISD = 1732m$.

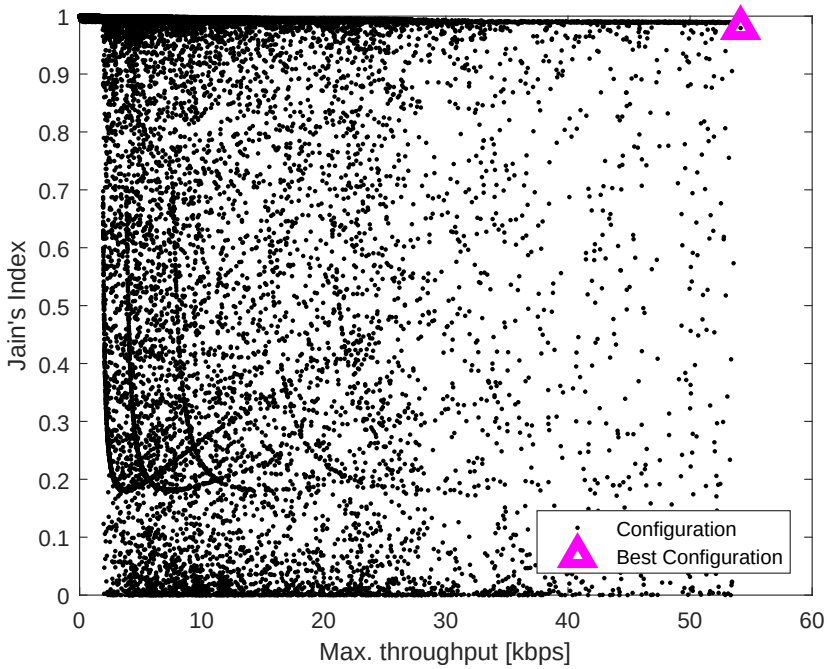

Fig. 4.7: Relation between the Jain's Index and the maximum throughput for $ISD = 1732m$.

By observing Fig. 4.8 it is possible to notice how the average success probability drops due to the lower coverage capability of the NB-IoT network. In particular there are much less configurations that guarantee an error rate lower than 10%,

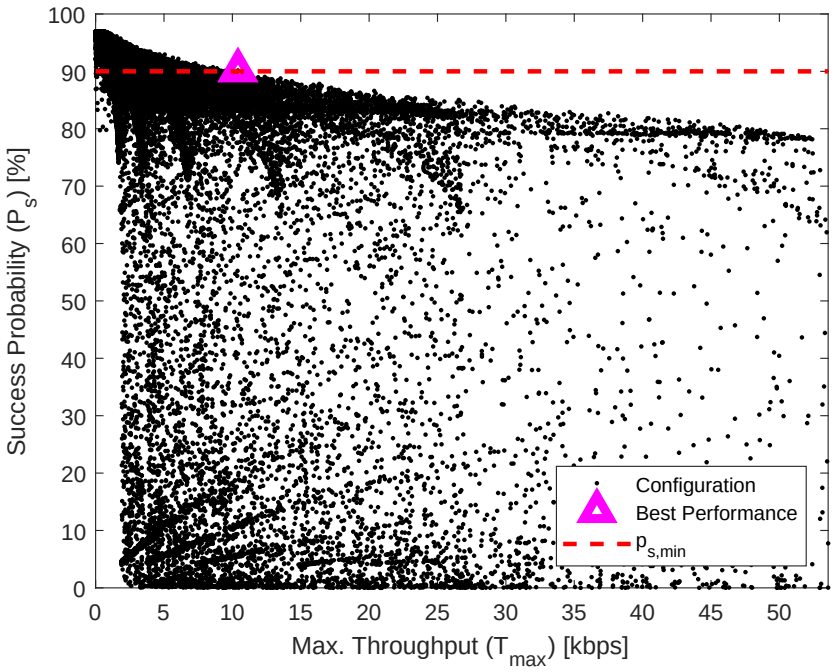

Fig. 4.8: Performance of a NB-IoT network with random generated configurations and $ISD = 3464m$.

	Best Performance (ISD= $3464m$)		
	N	***R***	***E***
p_c^{CONN}	42%	32%	17%
T_{max}	10.4 kbps		
P_s	90.2%		
JI	0.9		
	Configuration		
R_c	1	4	16
T_c	0.32 s	0.32 s	0.64 s
S_c	12	12	12
Th_1	-87 dBm		
Th_2	-105 dBm		

Table 4.4: Best performance and network configuration for $ISD = 3464m$.

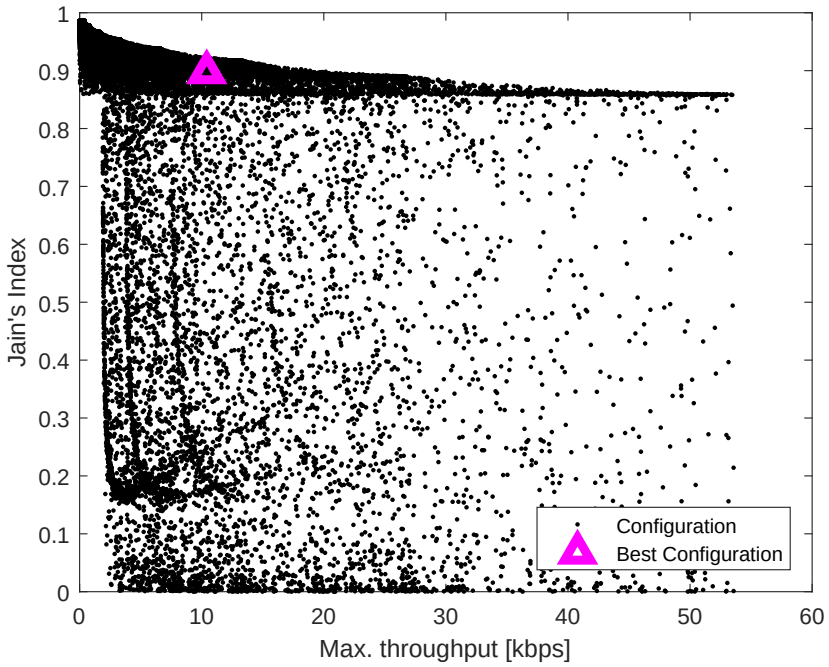

Fig. 4.9: Relation between the Jain's Index and the maximum throughput for $ISD = 3464m$.

configurations characterised by a lower maximum throughput. In order to guarantee a sufficient success rate, the number of repetitions configured should be higher on average, which causes a more redundant use of the radio resources and ultimately a lower throughput. In the best configuration it is possible to reach only 10.4 kbps with a success probability of 90.2%. In this scenario 17% of the devices, the ones in the worst coverage conditions, need to use 16 repetitions in order to be connected to the network.

Similarly, the Jain's Index is on average lower, as when the throughput is maximised, the devices are distributed more evenly into coverage classes characterised by different performance and behavior. Nevertheless the requirement of maintaining the error rate below a threshold has a similar impact also on the fairness which, in fact, is 0.9 in the aforementioned scenario.

In order to understand better the impact of each parameter, I performed the analysis reported in Fig. 4.10. Starting from a configuration characterised by poor

performance (the star marker, T_{max}= 25 kbps, P_s= 63%, ISD= 3464m), I tried to modify only one parameter, or a triplet of parameters, at a time. By increasing the number of repetitions (the solid line), I noticed that it is possible to increase the success probability with the drawback of a reduced throughput due to the less efficient use of the radio resources in the NPUSCH and viceversa.

The circles represent the performance obtainable by changing only Z_c; it is possible to improve both success rate and throughput although a clear scheme is not recognizable. In particular, considering the configurations placed in a horizontal line at the top (P_s= 85%), on the left we have configurations characterised by very large NPRACHs, enough to accommodate all the accesses but also very consuming in terms of radio resources so that the throughput cannot be very high. As we move on the right the NPRACHs sizes drop: they are still capable of process all the access requests but they start consuming less resources so that the throughput can be higher. Once reached the optimal NPRACH size, on the right side, the success probability start dropping and the NPRACH becomes the bottleneck of the system. The reason why the success probability cannot be higher than 85% is because of the limitation due to coverage issues which can be solved only by changing the number of repetitions.

Finally, by changing the decision thresholds (configurations represented by the dots) or by changing the way the devices are divided in the coverage classes, we can improve both the throughput and success rate. The optimal configuration consists in assigning the smallest number of devices possible to high number of repetitions classes if a lower number is sufficient to have coverage. In the top-left corner it is possible to notice how the success rate improves when many devices are configured with a high number of repetitions reaching coverage, though, with a lower throughput. Nevertheless, it is not possible to reach a success rate close to 100% because the NPRACHs should be dimensioned in order to accommodate the higher traffic in class Extreme; in this case the access success probability limits the performance.

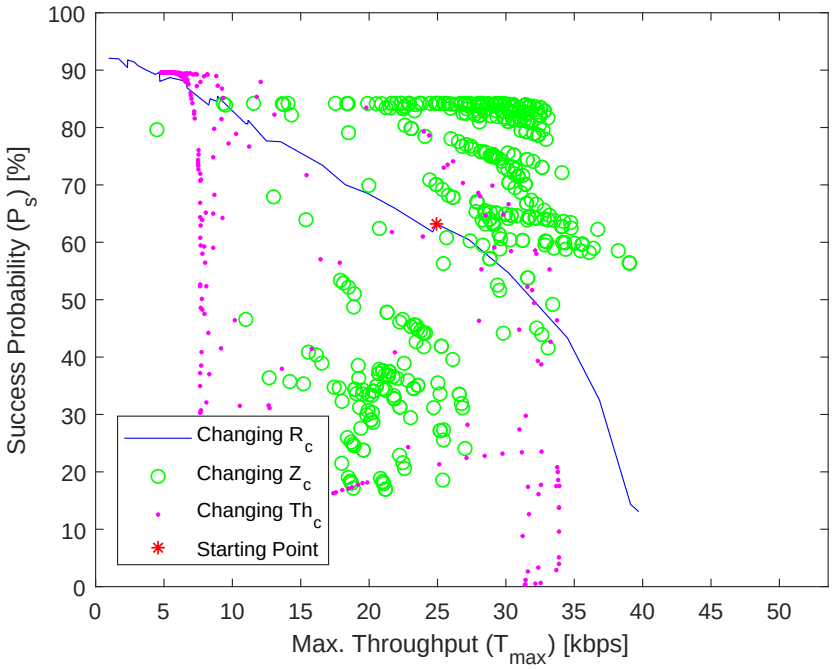

Fig. 4.10: Impact of the design parameters on the performance for $ISD = 3464m$.

Chapter 5

LoRa at Work

5.1 Deploying a Complete LoRaWAN Network

During the development of this thesis a LoRaWAN GW was deployed within the premises of the Engineering School in order to provide coverage within the building and to develop applications improving our understanding of this technology. This section describes the architecture of the resulting system and some applications that have been developed.

5.1.1 Network Architecture

According to the LoRaWAN specification, the system architecture is composed of a number of components starting from the ED and the GW already mentioned in Chapter 3.

Furthermore, the Network Server (NS) is the entity at the center of the star topology which receives and transmits packets through the GWs. It handles the datarate adaptation algorithm and all the MAC layer requests from the EDs. The Join requests are forwarded to the Join Server (JS) which handles the authentication of the devices in the network. Finally the Application Server (AS) handles the applications registered to the network; more specifically, all the traffic related to a specific application and set of devices is redirected through a specific interface.

For the network configured at the Engineering School we used a commercial gateway, the EMB-GW1301-O, produced by a local company, Embit srl[1]. This GW is based

[1]http://www.embit.eu/products/emb-gw1301gateway/

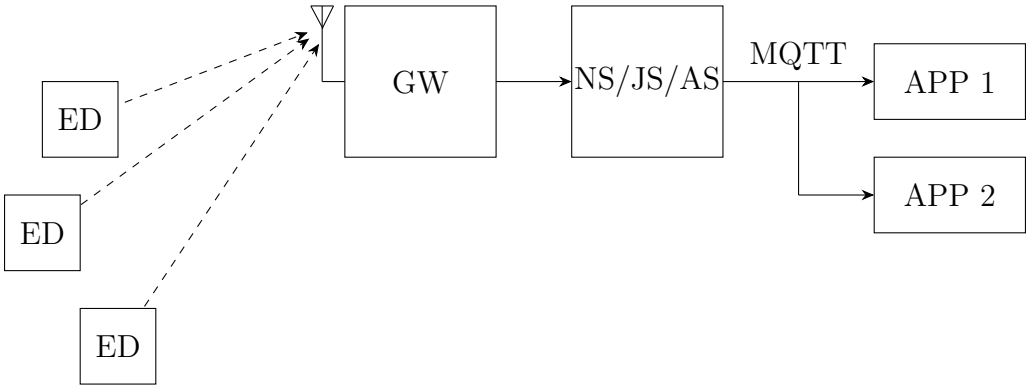

Fig. 5.1: Architecture of the LoRaWAN network deployed at engineering faculty.

on the SX1301 transceiver which was designed specifically by Semtech to support parallel decoding, allowing the GW to receive multiple packets on different channels and with different SFs at the same time.

The NS has been implemented by the Italian utility company A2A[2]. Their back-end, configurable through a web interface, implements all the aforementioned network functions: the NS, the AS and the JS. It is possible to create applications and register the devices to them through their DevEUI, an univocal address associated to the transceiver during the production phase. It is possible to access the device data through the Message Queue Telemetry Transport (MQTT) protocol.

If multiple GWs are connected to the A2A NS, it is possible to receive the traffic even if a device is in coverage of any other of these GWs. In fact, according to the LoRaWAN standard, the network should be transparent with respect to the actual deployment of the GW.

MQTT, working on top of Transmission Control Protocol (TCP)/IP protocol, has been designed to better support the sporadic nature of the communication happening in IoT applications compared to other protocols such as HyperText Transfer Protocol (HTTP). Being HTTP based on a query-reply mechanism, it would not be very efficient in case of an IoT application where uplink data is expected very sporadically. In such case, the application should periodically check for new data

[2]http://www.a2asmartcity.io/

creating a considerable amount of overhead traffic. On the other hand, MQTT is based on a subscribe-publish mechanism. The application subscribes to a "Topic", identified by a specific URL, which represents the source of information related to a particular aspect of the application, for instance all the packets related to a particular device. Once a new packet is actually transmitted, the MQTT broker implemented in the NS will notify to all the subscribed applications the presence of new data.

With an MQTT interface enabled, it is possible to design any kind of application able to retrieve and process the data produced by the sensors deployed. We decided to use Node-RED[3], a web-based tool which allows to process the data through an intuitive graphical user interface. Through this application it is also possible to create a multi-user system allowing the access to sensor data to different people while hiding, at the same time, the credentials used for the access to the A2A NS.

Finally, the network is able to support any kind of LoRaWAN compatible device, the ones used during our experiments are based on the EMB-LR1272E module, which utilise the SX1272 transceiver, although different kinds of boards have been used.

Fig. 5.1 summarises the aforementioned architecture.

5.1.2 Coverage Measurements

In order to test the capabilities of the network described in Section 5.1.1, I performed coverage measurements within the buildings of the Engineering School of University of Bologna. The target of this analysis is to check the possibility of providing coverage service to any other project or testbed deployed indoor.

The Engineering School is composed of two main buildings, both of them of four floors including the ground level. The surface covered by the building is approximatively a rectangle of 215×120 meters. Finally, close to the main entrance it is located the library tower, on top of which the GW has been placed at the south-east

[3]https://nodered.org/

corner at 71 meters of altitude with respect to the ground level. Fig. 5.2 shows a 3D representation of the School. For each point of measure, distributed across the floors of the School as depicted in Fig. 5.3, I transmitted 100 packets using the default SF configured by the network (SF7). We finally computed the average RSSI over all the packets received.

Fig. 5.3 shows a representation of the floors planimetry and the result of the measurements.

The coverage in most of the buildings is good (RSSI > -100 dBm) even in rooms that are located directly below the GW so that the signal has to cross multiple floors. Even with a close-to-sensitivity signal strength all the points studied are covered by the GW without the need of enabling the Adaptive Data Rate (ADR) function which would increase the coverage by increasing the SF with a lower datarate.

5.1.3 Application Example

In order to test the aforementioned measurement and, more generally, to test the whole system, I built a simple demo composed of five boards equipped with various kinds of sensors. The boards are based on the Arduino Zero, whereas the wireless modules used are the EMB-LR1272E, based on the SX1272 transceiver. The sensors used are three DHT11, capable of measuring the air temperature and relative humidity, one MQ135, able to measure the CO2 concentration, and one BH1750, able to measure the light intensity. The aim of this demo is to emulate on a small scale an application where the quality of the working conditions in a building are monitored through the measurements of these environmental indicators. Three devices have been deployed in our laboratory at the third floor of the School (Devices 5, 19 and 40), while the remaining two devices have been placed in two different offices at the second floor of the same building.

Through the web based User Interface created with Node-RED shown in Fig. 5.4, it is possible to monitor the current status of all the indicators in the three rooms. Also, the RSSI of all the devices is shown. In case no packets had been received in

Fig. 5.2: 3D representation of the Engineering School of University of Bologna and LoRaWAN GW deployment.

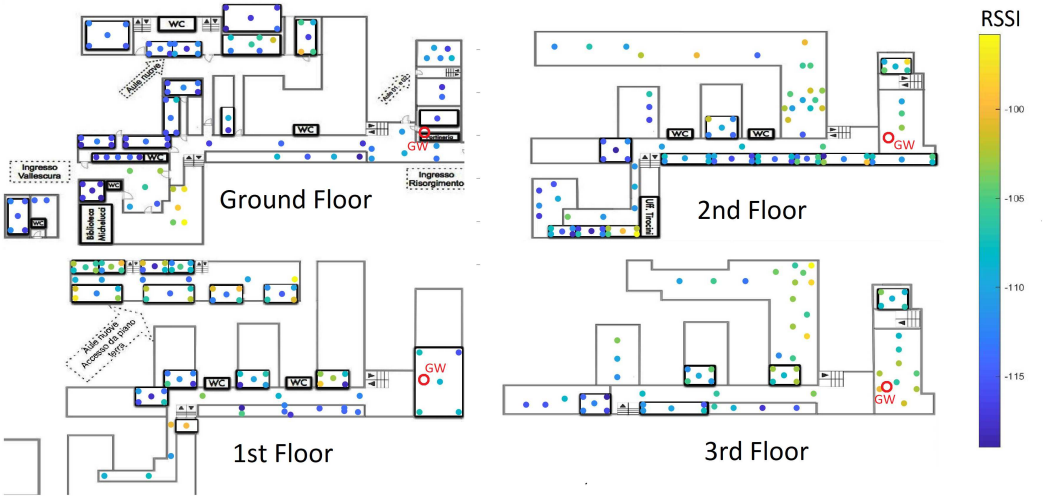

Fig. 5.3: Coverage measurements within Engineering School.

the last ten minutes, a notification would be shown stating that the corresponding device was disconnected.

As expected, considering the measurements described in Section 5.1.2, the coverage is fairly good in the three rooms monitored.

Through the User Interface it is also possible to set the packet generation rate for each device. When changed, a downlink message is sent to all devices with the

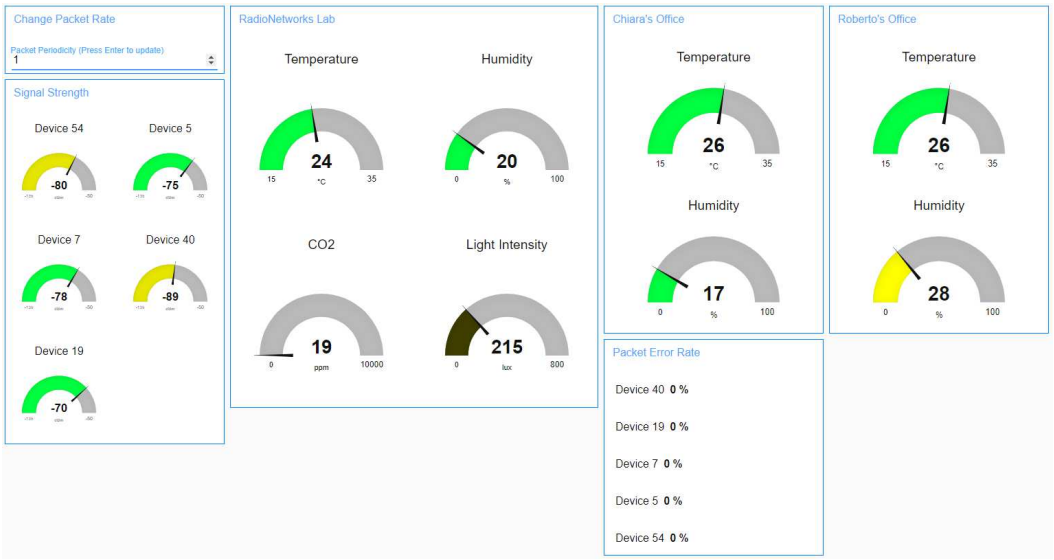

Fig. 5.4: Dashboard of the LoRaWAN example application.

new packet periodicity to be used from that moment. The devices are configured as Class A, therefore the downlink message is, first, stored in a buffer, then transmitted once an uplink packet is transmitted and the reception windows opened.

By setting the periodicity at the minimum, the total traffic received by the GW is roughly 66 packets per minute. According to the numerical results presented in Section 3.5, the capacity of a GW similar to the one we used in this demo is roughly 90 packets per minute per frequency channel, assuming P_L= 10 bytes. Since the GW is configured to use 8 channels, this demo consumes a very small amount of the radio resources available. In order to test the validity of the results presented, a system composed by more devices is needed, in order to generate a sufficient amount of traffic.

5.2 Smart Cities RIGERS Project

This section presents the implementation of a LoRa-based network, carried out in the framework of the RIGERS project. The RIGERS project is aimed at monitoring environmental conditions in residential and public buildings located in the "Saragozza" and "Navile" districts of Bologna. The reference region for the Saragozza

district is a rectangular area of 0.9 km × 1.8 km, with the gateway located at the median point of the longest side, while in the case of the Navile district it is a square area of side 0.6 km, with the gateway located in the south-west corner. Selected rooms of each building will be equipped with a multi-sensor platform hosting a LoRa transceiver to communicate the measured data to the gateway. In particular, each platform will be equipped with humidity, temperature, lighting, CO2 sensors and one globe thermometer. The RIGERS project is still ongoing and the final deployment has not been carried out yet.

In the view of the in-field implementation of the LoRa based pilot envisioned within RIGERS, in the following I present network-level results, obtained through the simulator described in Section 3.4 incorporating path-loss models obtained through measurement in the target areas.

For the simulation it has been considered G_{tot}= 4 dB, σ_S= 9 and a bandwidth of 125 kHz. In each scenario, either Saragozza or Navile districts, N buildings are randomly and uniformly chosen in the area of interest, and each building is assumed to host one multi-sensor board equipped with the LoRa device. Each board wakes up every five minutes and all its sensors take a sample. Then, once every hour (λ= 24 packets per day), the average of all the last measurements is transmitted. Since sensor measurements take 2 Bytes, each multisensor board generates P_L= 10 B to be transmitted to the gateway. Confirmed mode is also used and up to three retransmissions per packet are allowed. Since the gateway will be located on the roof of a building and the multisensor boards will be deployed indoor, I assume L_{add}= 12.5 dB to account for the additional loss due to the penetration of the wall.

We consider two cases: i) gateway equipped with a single receiver, which can be tuned to a specific channel and synchronised on a specific SF value; ii) gateway equipped with different receivers, such that it is able to decode signals transmitted using different SF (again a single channel is considered). The first case refers to the receiver that will be used in the RIGERS project, while the second case refers to a commercial LoRaWAN gateway. In the second case, all nodes start using SF= 7 and then, every two retransmissions, SF is increased by one to mitigate coverage

issues (curves related to this case are denoted as "variable SF" in Fig. 5.5). After three simulated hours, SF is reset to 7.

Fig. 5.5(a) and Fig. 5.5(b) report the percentage of packets correctly received by the gateway (packet success rate - P_s), as a function of the number of buildings deployed, N, for the Navile and Saragozza districts, respectively. Both the cases of variable and fixed SF, when considering different values of SF, are reported in the figures.

In the case of Navile, when setting low values of SF, the network is limited by connectivity and the P_s slightly depends on N. Indeed, the ideal (when shadowing is not present) transmission range is within 0.3 km (obtained when setting SF= 7) and 0.8 km (for the case SF= 12), while the maximum distance covered in the scenario is 0.85 km. This connectivity problem is mitigated when setting SF= 12, allowing to reach more buildings (lower receiver sensitivity); however, as SF increases, the T_A increases as well (1.18 s when SF= 12, versus 0.05 s when SF=7), resulting in a larger collision probability and a reduction of the P_s when N increases. Since nodes use a simple ALOHA protocol to access the channel, an increase in airtime brings to a performance worsening in interference limited scenarios. In conclusion, SF= 10 is the best case, allowing a good trade-off between connectivity and collision issues, and allowing to achieve a P_s larger then 90% for up to 400 nodes/buildings. In this scenario, the strategy suggested by the standard to dynamically set SF (variable SF) does not allow to obtain the best performance. This is due to the fact that the scenario is limited by connectivity, therefore many nodes do not receive the ACK, increase SF and after some transmissions many nodes tend to use SF= 12, which is not the best value because of collisions (see the curve SF= 12). Finally, note that the trends of the curves reported in this figure are very similar to those of the curves reported in Figure 9 of [43]: in particular, a weak dependence of the packet delivery ratio on the number of devices is observed also in [43] in case of connectivity issues (almost flat behavior of the curve related to SF= 7). Moreover, also in [43] the choice SF= 12 appears the best solution when few nodes are present, but it becomes the worst case when increasing the traffic generated, because of collisions.

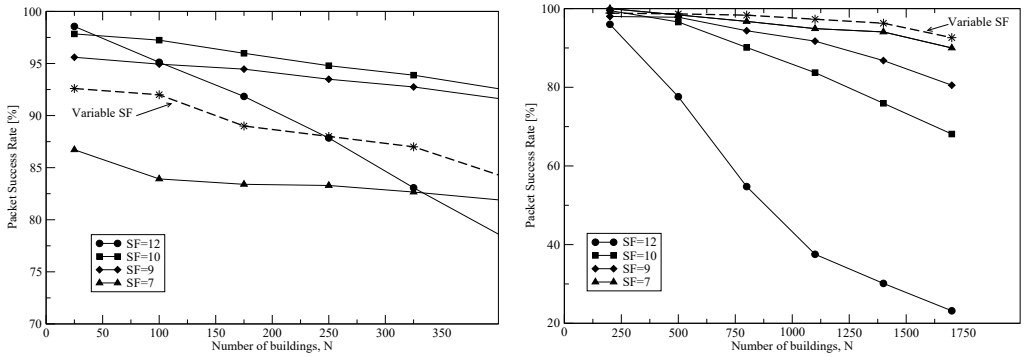

(a) Navile District.

(b) Saragozza District.

Fig. 5.5: Packet success rates vs. number of buildings in both the Navile and Saragozza districts.

As far as Saragozza is concerned, being the power decay index lower, there are not connectivity issues: a P_s of 100% is obtained for low values of N. As a result, the P_s decreases with N for all values of SF and SF= 7 is the value that maximises the success rate, since it is characterised by the lowest value of airtime. In this case, if the application requires a minimum PSR of 90%, the LoRa gateway is able to serve up to approximately 1700 buildings. In this scenario, instead, the use of a variable SF allows to maximise the performance, because less connectivity issues are present and only few nodes increase SF. As a result, performance is better than in the case SF= 7, since more nodes can reach the gateway, but just few nodes increase SF, therefore collisions are still mitigated.

In the above figures, the standard deviation of the P_s is always below 2%.

Chapter 6
Conclusion

We have assessed the capacity of a LoRaWAN network for a broad range of use cases of interest, specifically focusing on rural environments. This has been achieved through an experimental assessment of the link-level characteristics of the system, followed by a system-level simulation implementing all LoRaWAN specifications.

With reference to each use case, network capacity has been defined based on requirements on the success probability and the transmission rates of nodes.

Two separate scenarios have been analyzed, of very different size. In the smaller case, where one single gateway is used, as might be expected I found that optimal configuration of the network is achieved by setting lower values of SF, using confirmed mode. In the case of a larger scenario, I analyzed the network capacity obtained with one or more gateways. In the former case, as expected, network capacity is severely degraded, due to the need to use larger (and less efficient) values of SF; in the latter, a significant improvement is found.

The analysis performed provides useful insights for the development of LoRaWAN networks.

This thesis also presented a detailed description of the main features of NB-IoT and the procedures for data transmission and reception with related sources of latency. The thesis discussed how the configuration of network parameters affects the latency performance of NB-IoT. It was provided an analysis in terms of capacity considering real-life use cases for sensor reporting, and analyzed how NB-IoT might be tuned to improve its capacity. We further analyzed the performance on the downlink direction focusing on a firmware update use case, studying the benefits of the multicast transmission mode recently introduced in Rel. 14.

The thesis presented also a mathematical model describing a large network implementing the same application with devices deployed in different connectivity conditions; in particular, two scenarios where the operator decides to deploy the NB-IoT sites at different distances among them, have been considered. We provided an analysis in terms of maximum throughput, success probability and service fairness, considering randomly generated configurations of some design parameters, with the objective of finding the one maximizing the performance. Apart from providing an estimation of the performance achieved in different scenarios, this thesis provides an useful methodology for the design space exploration. In fact, most of the random configurations lead to a very poor performance; thus, a smart selection of these parameters can lead to an important improvement.

Moreover, this analysis shows that in the deployment scenario considered, and with NB-IoT deployed in one site every 12 LTE sites, NB-IoT is able to provide good coverage to all the UEs and that it is possible to disable some coverage classes to save radio resources. With NB-IoT sites deployed more sparsely, coverage becomes a major issue and the design parameters should be optimised in order to guarantee coverage while minimizing the number of repetitions used and guarantee a high access success probability while the capacity of the NPRACH is minimised.

In the end LoRaWAN and NB-IoT, among all the other technologies present in the market, provide very different performance, and it is expected that both of them will be used for the most appropriate kind of application. The future of these technologies will strongly depend on the business model applied by the operators. LoRaWAN may still be suited for stand-alone applications or it may be integrated in larger networks managed by operators, whereas the amount of devices employing NB-IoT will depend on the subscription cost.

6.1 Future Works

This thesis is mainly focused on the analysis of these two technologies. The most immediate continuation of this work may consists in the application of these models

to optimization problems aiming to the maximization of the network performance. Regarding LoRaWAN, some works in this direction are already present, while the complexity of NB-IoT makes this topic mostly unexplored.

It may be interesting to apply the peculiarities of both technologies in novel communication paradigms, such as Device to Device (D2D) communications or Unmanned Aerial Vehicle (UAV) aided networks. The latter scenario is expected to become a solution to improve coverage at the cell edge or during abnormal peaks of traffic in beyond-5G networks.

Finally, these technologies are still not well known to the maker community which may considerably increase the market size. Research activities should focus in providing open source resources. Also, it is important to perform dissemination activities in order to spread the knowledge derived by the use of these technologies.

In the last year we organised an Hackathon[1] at University of Bologna where more than 80 participants challenged themselves in building a working IoT application employing Arduino boards and the LoRaWAN network described in Section 5.1. An event of this kind, supported by a technical committee composed of persons representing the most important companies in this field, has the potential to make people aware of the new possibilities given by IoT.

[1]Long Range IoT Hackathon 2018, http://longrangeiothackathon.org/

Bibliography

[1] Link Labs. (2018) What is LoRa? A Technical Breakdown. [Online]. Available: https://www.link-labs.com/blog/what-is-lora vii, 28

[2] 3GPP. (2015) TS 45.820 - cellular system support for ultra-low complexity and low throughput Internet of Things (CIoT). [Online]. Available: https://portal.3gpp.org ix, 6, 7, 12, 63, 66, 77

[3] Andreas F. Molisch, "The Okumura-Hata model," in *Wireless Communications*. John Wiley and Sons, Ltd, 2005, ch. Appendix 7.A. ix, 5, 7

[4] 3GPP. (2013) TS 36.888 - Study on provision of low-cost Machine-Type Communications (MTC) User Equipments (UEs) based on LTE. [Online]. Available: https://portal.3gpp.org ix, 7, 8

[5] GSMA, "3GPP low power wide area technologies, GSMA white paper," Tech. Rep., October 2016. ix, 11, 12, 20, 21, 24, 42, 47, 55, 61

[6] Ericsson, "Ericsson mobility report," Tech. Rep., November 2016. ix, 7, 11, 12, 19, 24, 42, 47

[7] (2013) SmartSantander, future internet research and experimentation. [Online]. Available: http://www.smartsantander.eu/ ix, 13, 24

[8] 3GPP. (2017) TS 36.211 - Evolved Universal Terrestrial Radio Access (E-UTRA) Physical channels and modulation. [Online]. Available: https://portal.3gpp.org ix, 48, 58, 59, 62, 77

[9] C. Goursaud and J.-M. Gorce, "Dedicated networks for IoT : PHY / MAC state of the art and challenges," *EAI endorsed transactions on Internet of Things*, Oct. 2015. [Online]. Available: https://hal.archives-ouvertes.fr/hal-01231221 1, 26

[10] Z. Dawy, W. Saad, A. Ghosh, J. G. Andrews, and E. Yaacoub, "Toward Massive Machine Type Cellular Communications," *IEEE Wireless Communications*, vol. 24, no. 1, pp. 120–128, February 2017. 1

[11] M. R. Palattella, M. Dohler, A. Grieco, G. Rizzo, J. Torsner, T. Engel, and L. Ladid, "Internet of Things in the 5G Era: Enablers, Architecture, and Business Models," *IEEE Journal on Selected Areas in Communications*, vol. 34, no. 3, pp. 510–527, March 2016. 1

[12] H. Wang and A. O. Fapojuwo, "A Survey of Enabling Technologies of Low Power and Long Range Machine-to-Machine Communications," *IEEE Communications Surveys Tutorials*, vol. 19, no. 4, pp. 2621–2639, Fourthquarter 2017. 1

[13] Orange, "LoRa Device Developer Guide," Tech. Rep., April 2016. 2

[14] "What the internet of things (IoT) needs to become a reality," Freescale, ARM, Tech. Rep., 2014. 20

[15] M. Aref and A. Sikora, "Free space range measurements with semtech LoRa™technology," in *Wireless Systems within the Conferences on Intelligent Data Acquisition and Advanced Computing Systems: Technology and Applications (IDAACS-SWS), 2014 2nd International Symposium on*, Sept 2014, pp. 19–23. 25

[16] J. Petajajarvi, K. Mikhaylov, A. Roivainen, T. Hanninen, and M. Pettissalo, "On the coverage of LPWANs: range evaluation and channel attenuation model for lora technology," in *ITS Telecommunications (ITST), 2015 14th International Conference on*, Dec 2015, pp. 55–59. 25

[17] L. Li, J. Ren, and Q. Zhu, "On the application of LoRa LPWAN technology in sailing monitoring system," in *2017 13th Annual Conference on Wireless On-demand Network Systems and Services (WONS)*, Feb 2017, pp. 77–80. 25

[18] W. San-Um, P. Lekbunyasin, M. Kodyoo, W. Wongsuwan, J. Makfak, and J. Kerdsri, "A long-range low-power wireless sensor network based on U-LoRa

technology for tactical troops tracking systems," in *2017 Third Asian Conference on Defence Technology (ACDT)*, Jan 2017, pp. 32–35. 26

[19] V. A. Stan, R. S. Timnea, and R. A. Gheorghiu, "Overview of high reliable radio data infrastructures for public automation applications: LoRa networks," in *2016 8th International Conference on Electronics, Computers and Artificial Intelligence (ECAI)*, June 2016, pp. 1–4. 26

[20] B. Sikken. (2016) Decoding LoRa. [Online]. Available: https://revspace.nl/DecodingLora 26

[21] M. Knight and B. Seeber, "Decoding LoRa: Realizing a modern LPWAN with SDR," 2016. 26

[22] M. Bor, J. Vidler, and U. Roedig, "LoRa for the Internet of Things," in *Proceedings of the 2016 International Conference on Embedded Wireless Systems and Networks*, ser. EWSN '16, 2016, pp. 361–366. 26

[23] O. Georgiou and U. Raza, "Low power wide area network analysis: Can LoRa scale?" *IEEE Wireless Communications Letters*, vol. PP, no. 99, pp. 1–1, 2017. 26

[24] K. Mikhaylov, J. Petaejaejaervi, and T. Haenninen, "Analysis of capacity and scalability of the lora low power wide area network technology," in *European Wireless 2016; 22th European Wireless Conference*, May 2016, pp. 1–6. 26

[25] F. Adelantado, X. Vilajosana, P. Tuset-Peiró, B. Martínez, and J. Melià, "Understanding the limits of lorawan," *CoRR*, vol. abs/1607.08011, 2016. [Online]. Available: http://arxiv.org/abs/1607.08011 26

[26] M. C. Bor, U. Roedig, T. Voigt, and J. M. Alonso, "Do LoRa low-power wide-area networks scale?" in *Proceedings of the 19th ACM International Conference on Modeling, Analysis and Simulation of Wireless and Mobile Systems*, ser. MSWiM '16. New York, NY, USA: ACM, 2016, pp. 59–67. [Online]. Available: http://doi.acm.org/10.1145/2988287.2989163 26

[27] A. J. Wixted, P. Kinnaird, H. Larijani, A. Tait, A. Ahmadinia, and N. Strachan, "Evaluation of LoRa and LoRaWAN for wireless sensor networks," in *2016 IEEE SENSORS*, Oct 2016, pp. 1–3. 27

[28] LoRa Alliance, "LoRaWAN specification," January 2015. 28

[29] Semtech, "AN1200.22 LoRa Modulation Basics," May 2015. 28

[30] Semtech, "Datasheet SX1272/73 - 860 MHz to 1020 MHz Low Power Long Range Transceiver," March 2015. 28

[31] C. Gezer, C. Buratti, and R. Verdone, "Capture effect in IEEE 802.15.4 networks: Modelling and experimentation," pp. 204–209, May 2010. 30

[32] M. Gudmundson, "Correlation model for shadow fading in mobile radio systems," *Electronics Letters*, vol. 27, no. 23, pp. 2145–2146, Nov 1991. 35

[33] Y. P. E. Wang, X. Lin, A. Adhikary, A. Grovlen, Y. Sui, Y. Blankenship, J. Bergman, and H. S. Razaghi, "A Primer on 3GPP Narrowband Internet of Things," *IEEE Communications Magazine*, vol. 55, no. 3, pp. 117–123, March 2017. 48

[34] 3GPP. (2017) TS 36.321 - Evolved Universal Terrestrial Radio Access (E-UTRA) Medium Access Control (MAC) protocol specification. [Online]. Available: https://portal.3gpp.org 48, 61

[35] ——. (2017) TS 36.213 - Evolved Universal Terrestrial Radio Access (E-UTRA) Physical layer procedures. [Online]. Available: https://portal.3gpp.org 48, 56, 59, 61, 62

[36] ——. (2017) TS 36.331 - Evolved Universal Terrestrial Radio Access (E-UTRA) Radio Resource Control (RRC) protocol specification. [Online]. Available: https://portal.3gpp.org 48, 58, 63

[37] J. Schlienz and D. Raddino, "Narrowband Internet of Things," White Paper, August 2016. 48

[38] R. Ratasuk, N. Mangalvedhe, Y. Zhang, M. Robert, and J. Koskinen, "Overview of narrowband iot in lte rel-13," in *2016 IEEE Conference on Standards for Communications and Networking (CSCN)*, Oct 2016, pp. 1–7. 48, 55

[39] N. Mangalvedhe, R. Ratasuk, and A. Ghosh, "NB-IoT deployment study for low power wide area cellular IoT," in *2016 IEEE 27th Annual International Symposium on Personal, Indoor, and Mobile Radio Communications (PIMRC)*, Sept 2016, pp. 1–6. 48

[40] A. Adhikary, X. Lin, and Y. P. E. Wang, "Performance Evaluation of NB-IoT Coverage," in *2016 IEEE 84th Vehicular Technology Conference (VTC-Fall)*, Sept 2016, pp. 1–5. 53, 56, 61

[41] Y. D. Beyene, R. Jantti, K. Ruttik, and S. Iraji, "On the Performance of Narrow-Band Internet of Things (NB-IoT)," in *2017 IEEE Wireless Communications and Networking Conference (WCNC)*, March 2017, pp. 1–6. 66, 72

[42] 3GPP. (2011) TS 37.868 - Study on RAN Improvements for Machine-type Communications. [Online]. Available: https://portal.3gpp.org 72

[43] F. Van-Den-Abeele, J. Haxhibeqiri, I. Moerman, and J. Hoebeke, "Scalability analysis of large-scale LoRaWAN networks in NS-3," *IEEE Internet of Things Journal*, vol. 4, no. 6, pp. 2186–2198, Dec 2017. 91

Publications

The research reported in this thesis resulted in the publications at international conferences and journals summarised below.

[44] L. Feltrin, S. Mijovic, C. Buratti, A. Stajkic, E. Vinciarelli, R. Verdone, and R. D. Bonis, "Performance Evaluation of LoRa Technology: Experimentation and Simulation," in *EuCNC 2016, Athens, Greece*, June 2016.

[45] L. Feltrin, A. Marri, M. Paffetti, and R. Verdone, "Preliminary evaluation of NB-IOT technology and its capacity," in *Dependable Wireless Communications and Localization for the IoT Workshop, Graz, Austria*, Sept 2017.

[46] L. Feltrin, M. Condoluci, T. Mahmoodi, M. Dohler, and R. Verdone, "NB-IoT: Performance Estimation and Optimal Configuration," in *European Wireless 2018; 24th European Wireless Conference*, May 2018, pp. 1–6.

[47] G. Pasolini, C. Buratti, L. Feltrin, F. Zabini, R. Verdone, O. Andrisano, and C. D. Castro, "Smart City Pilot Project Using LoRa," in *European Wireless 2018; 24th European Wireless Conference*, May 2018, pp. 1–6.

[48] G. Pasolini, C. Buratti, L. Feltrin, F. Zabini, C. De Castro, R. Verdone, and O. Andrisano, "Smart City Pilot Projects Using LoRa and IEEE802.15.4 Technologies," *Sensors*, vol. 18, no. 4, 2018. [Online]. Available: http://www.mdpi.com/1424-8220/18/4/1118

[49] L. Feltrin, C. Buratti, E. Vinciarelli, R. D. Bonis, and R. Verdone, "LoRaWAN: Evaluation of Link- and System-Level Performance," *IEEE Internet of Things Journal*, vol. 5, no. 3, pp. 2249–2258, June 2018.

[50] L. Feltrin, G. Tsoukaneri, M. Condoluci, C. Buratti, T. Mahmoodi, M. Dohler, and R. Verdone, "NarrowBand-IoT: A Survey on Downlink and Uplink Perspec-

tives," *Accepted for publication at IEEE Wireless Communication Magazine*, Jan 2018.

[51] L. Feltrin, M. Condoluci, T. Mahmoodi, M. Dohler, and R. Verdone, "NB-IoT: Performance Estimation and Optimal Configuration," *Submitted to IEEE Internet of Things Journal*, Nov 2018.

Acknowledgements

Questi ultimi tre anni di dottorato sono volati. Sono stati anni densi di esperienze e viaggi eccitanti. Ho avuto modo di crescere sul piano professionale e di imparare a fare ricerca. Insomma, è stata un'esperienza sicuramente positiva. Per questo devo ringraziare Roberto e Chiara che mi hanno guidato in questo percorso non solo con grande capacità tecnica, ma anche con una grande umanità e simpatia. Questi tre anni rimarranno un bellissimo ricordo grazie anche alle persone eccezionali con le quali li ho condivisi, Andrea, Stefan, Colian, Lucia, Riccardo, Danilo, Silvia e tanti altri.

Il tempo che ho passato a Bologna non è stato di solo lavoro. Dopo decine di serate insieme e centinaia di momenti di quotidianità mi sono sentito come a casa. Per questo, grazie di cuore Luca, Manuel, Marina, Myriam, Sara, Chiara, Gloria, Fainot, Davide, Eleonora e Giada. Grazie anche a Giulia, una grande amica con la quale ho scoperto la passione per la salsa, una piacevole sorpresa anche per me.

Oggi sono qui anche grazie agli amici di una vita, con i quali sono cresciuto nella mia Forlì. Sono troppi da elencare i momenti passati insieme, ma ognuno di voi ha un posto speciale nei miei ricordi. La mia ultima serata a Forlì prima di partire per la Svezia è un ricordo davvero speciale. Grazie Filippo, Medri, Celli, Cippo, Supra, Bikash, Cele e tutti gli altri. Un grazie speciale anche a te Giada, i momenti insieme sono stati troppo pochi ma saranno impressi dentro di me per sempre.

Ultimi ma non meno importanti i miei genitori. Oggi sono la persona che sono grazie a loro. Mi hanno trasmesso la voglia di scoprire il mondo con curiosità, umiltà ed impegno. Mi hanno insegnato che la vita va presa con il sorriso ed un pizzico di ironia. Questo è il contributo più importante di tutti. Grazie di cuore.